Chiral asymmetry in propagation of soliton defects in crystalline backgrounds

Adrián Arancibia[*] and Mikhail S. Plyushchay[†]

Departamento de Física, Universidad de Santiago de Chile, Casilla 307, Santiago 2, Chile
(Received 3 August 2015; published 5 November 2015)

By applying Darboux-Crum transformations to a Lax pair formulation of the Korteweg–de Vries (KdV) equation, we construct new sets of multisoliton solutions to it as well as to the modified Korteweg–de Vries (mKdV) equation. The obtained solutions exhibit a chiral asymmetry in the propagation of different types of defects in crystalline backgrounds. We show that the KdV solitons of pulse and compression modulation types—which support bound states in, respectively, semi-infinite and finite forbidden bands in the spectrum of the perturbed quantum one-gap Lamé system—propagate in opposite directions with respect to the asymptotically periodic background. A similar but more complicated picture also appears for multi-kink-antikink mKdV solitons that propagate with a privileged direction over the topologically trivial or topologically nontrivial crystalline background depending on the position of the energy levels of the trapped bound states in the spectral gaps of the associated Dirac system. An exotic $N = 4$ nonlinear supersymmetric structure incorporating Lax-Novikov integrals of a pair of perturbed Lamé systems is shown to underlie the Miura-Darboux-Crum construction. It unifies the KdV and mKdV solutions, detects the defects and distinguishes their types, and identifies the types of crystalline backgrounds.

I. INTRODUCTION

Nonlinear integrable systems play an important role in a variety of areas of physics and its applications [1–8]. A Lax pair formulation in particular cases of the Korteweg–de Vries (KdV) and modified Korteweg–de Vries (mKdV) equations relates their soliton, kink, kink-antikink, and crystalline type solutions with reflectionless and finite-gap systems of quantum mechanics [9–11]. This formulation for the KdV and mKdV systems includes, respectively, the stationary Schrödinger and Dirac equations (the latter with a scalar potential) as the eigenstate equation.

The inverse scattering method allows one to construct soliton solutions for the KdV equation in an analytical form for the asymptotically free, homogeneous boundary conditions. On the other hand, such analytic solutions can also be constructed by exploiting the covariance of the Lax pair under Darboux transformations and their generalization in the form of Darboux-Crum transformations. From the spectral point of view, these transformations correspond to adding soliton defects by means of introducing bound states into the spectrum of the initial potential [10].

Recently in Ref. [12], by employing Darboux-Crum transformations, we constructed a generalization of reflectionless potentials by introducing soliton defects into the periodic (crystalline) background of the one-gap Lamé system,

$$U_{\text{Lamé}}(x) = 2k^2 \text{sn}^2(x|k) + \text{const.} \qquad (1.1)$$

As a result, we obtained one-gap potentials for the Schrödinger system with an arbitrary number of bound states in the lower and intermediate forbidden bands, which are trapped by the soliton defects.

Using a relation between Darboux transformations and supersymmetric quantum mechanics, it was also possible to construct finite-gap Dirac (Bogoliubov–de Gennes) Hamiltonian operators, in which scalar potentials carry perturbations of the kink and kink-antikink types introduced into the different crystalline backgrounds.

One such periodic background corresponds to the superpotential of the form [13–16]

$$V^{\text{KC}}(x) = \frac{d}{dx} \log \text{dn}(x|k) = -k^2 \frac{\text{cn}(x|k)\text{sn}(x|k)}{\text{dn}(x|k)}. \qquad (1.2)$$

This finite-gap Dirac scalar potential appeared as a solution in the Gross-Neveu model with a discrete chiral symmetry [17,18], and was identified there as the kink crystal. In the QCD framework, the kink crystal can be considered as the phase corresponding to the crystalline color superconductor [19], that is, the QCD analog of the Larkin-Ovchinnikov-Fulde-Ferrell phase in the context of electron superconductivity [20,21]. The kink crystal type solution (1.2) also found some applications in the physics of conducting polymers [22,23]. In the construction from Ref. [12], the Dirac Hamiltonian operator with the perturbed scalar potential of the form (1.2) possesses a spectrum having a central allowed band between the conduction band and

*adaran.phi@gmail.com
†mikhail.plyushchay@usach.cl

the Dirac sea, and the bound states appear there symmetrically in both forbidden bands (gaps).

There is yet another possibility for asymptotic behavior in the form of the kink-antikink, V^{KA}, (or, antikink-kink, V^{AK}) crystal [16],

$$V^{KA}(x) = Z(x + \beta|k) - Z(x|k) - z(\beta|k),$$
$$V^{AK}(x) = -V^{KA}(x), \tag{1.3}$$

which was found as a solution in the Gross-Neveu model with a bare mass term [24]. It allowed one to obtain scalar potentials with two permitted bands between the Dirac sea and conduction band, with an arbitrary number of bound states in the central and/or other two forbidden bands. Here $z(\beta|k)$ is a constant given in terms of the Jacobi zeta and elliptic functions, $z(\beta|k) = Z(\beta + i\mathbf{K}'|k) + i\frac{\pi}{2\mathbf{K}} = Z(\beta|k) + cn(\beta|k)dn(\beta|k)/sn(\beta|k)$. An additional change of the global topology of the Dirac scalar potential provided us with reflectionless kink-antikink perturbations over the kink type crystalline background.

A natural question we address in this paper is the following: how can the dependence on time be "reconstructed" for the finite-gap Schrödinger and Dirac crystalline potentials with defects, found in Ref. [12], so that they will be solutions for the KdV and mKdV equations? We refer here to the evolution parameter in the corresponding nonlinear integrable systems; from the perspective of the eigenvalue problems, it is associated with the isospectral deformation of the potentials. Answering this question, we reveal a phenomenon of a chiral asymmetry in the propagation of different types of soliton defects in crystalline backgrounds, which (as we believe) could be interesting, particularly from the point of view of applications.

The paper is organized as follows. In Sec. II (which is a very brief review), we consider the Lax pair formulation for the KdV equation, discuss its Darboux covariance, and apply the Darboux and Darboux-Crum transformations to obtain multisoliton solutions for the KdV equation. Section III is devoted to the construction of solutions to the auxiliary problem corresponding to the Lax pair with the one-gap Lamé potential taken as the stationary, periodic cnoidal solution to the KdV equation. On the basis of the solutions to the auxiliary problem, in Sec. IV we construct solutions to the KdV equation by employing Darboux-Crum transformations. In this way we obtain the KdV solutions that describe the propagation of solitons of the potential well (pulse) and compression modulation types in the background of an asymptotically periodic cnoidal wave. We also discuss there the issue of the velocities of the defects. In Sec. V, we first show how the Miura and Darboux-Crum transformations together with the Galilean symmetry of the KdV equation can be employed for the construction of solutions to the mKdV equation on the basis of the KdV solutions. Then we discuss the exotic $N = 4$

nonlinear supersymmetric structure incorporating Lax-Novikov integrals of a pair of perturbed Lamé systems. This supersymmetry underlies the Miura-Darboux-Crum construction and unifies the KdV and mKdV solutions. In Sec. VI we first discuss briefly the asymptotically free mKdV solutions corresponding to the multi-kink-antikink solitons propagating over the kink or kink-antikink background. Then we construct a much more rich set of multi-kink-antikink soliton solutions for the mKdV equation which propagate over the topologically trivial or topologically nontrivial crystalline backgrounds. Finally, Sec. VII is devoted to the discussion and outlook.

II. LAX PAIR FOR THE KdV EQUATION, DARBOUX TRANSFORMATIONS, AND MULTISOLITON SOLUTIONS

A. Auxiliary spectral problem for the KdV equation

Consider a linear system

$$L\phi = \lambda\phi, \qquad \frac{\partial\phi}{\partial t} = P\phi \tag{2.1}$$

for a function $\phi = \phi(x, t, \lambda)$. It is assumed that L and P are some (in general, matrix) differential operators in the spatial coordinate $x \in \mathbb{R}$ with coefficients that can also depend on the evolution parameter t. If the evolution in t generated by P is isospectral, $d\lambda/dt = 0$, then the condition of consistency for the system (2.1) reduces to the Lax equation

$$\frac{\partial L}{\partial t} = [P, L]. \tag{2.2}$$

For the choice of the Lax pair in the form of differential operators

$$L = -\partial_x^2 + u, \tag{2.3}$$

$$P = -4\partial_x^3 + 6u\partial_x + 3u_x, \tag{2.4}$$

Eq. (2.2) reduces to the Korteweg–de Vries equation for the scalar field $u = u(x, t)$,

$$u_t = 6uu_x - u_{xxx}. \tag{2.5}$$

B. Darboux covariance of the KdV equation

The system of equations corresponding to the Lax pair (2.3) and (2.4),

$$(-\partial_x^2 + u)\Psi(x, t, \lambda) = \lambda\Psi(x, t, \lambda), \tag{2.6}$$

$$\frac{\partial}{\partial t}\Psi(x, t, \lambda) = (-4\partial_x^3 + 6u\partial_x + 3u_x)\Psi(x, t, \lambda), \tag{2.7}$$

is covariant under Darboux transformations [10],

$$u(x,t) \to u_1(x,t) = u(x,t) - 2(\log \Psi(x,t,\lambda_1))_{xx}, \quad (2.8)$$

$$\Psi(x,t,\lambda) \to \Psi_1(x,t,\lambda) = \frac{W(\Psi(x,t,\lambda_1), \Psi(x,t,\lambda))}{\Psi(x,t,\lambda_1)}, \quad (2.9)$$

where W is the Wronskian, $W(f,g) = fg_x - f_xg$. This follows from the observation that if Eqs. (2.6) and (2.7) are fulfilled for $\Psi(x,t,\lambda)$, and $\Psi(x,t,\lambda_1)$ satisfies the same equations with λ substituted for λ_1, then $\Psi_1(x,t,\lambda)$ obeys the equations (2.6) and (2.7) with $u(x,t)$ substituted for $u_1(x,t)$. As a consequence, if $u(x,t)$ is a solution of the KdV equation (2.5), then $u_1(x,t)$ obeys the same equation.

This result can be extended for a finite sequence of consecutive Darboux transformations,

$$u(x,t) \to u_m(x,t)$$
$$= u(x,t) - 2(\log W(\Psi(x,t,\lambda_1), ..., \Psi(x,t,\lambda_m)))_{xx}, \quad (2.10)$$

$$\Psi(x,t,\lambda) \to \Psi_m(x,t,\lambda)$$
$$= \frac{W(\Psi(x,t,\lambda_1), ..., \Psi(x,t,\lambda_m), \Psi(x,t,\lambda))}{W(\Psi(x,t,\lambda_1), ..., \Psi(x,t,\lambda_m))}, \quad (2.11)$$

which is known as the Darboux-Crum transformation of order m [10]. For the sake of simplicity of notation, the dependence of $u_m(x,t)$ as well as of $\Psi_m(x,t,\lambda)$ on the spectral parameters $\lambda_1, ..., \lambda_m$ is not shown explicitly.

One can define a first-order differential operator A_1 in terms of the function $\Psi(x,t,\lambda_1)$ that underlies the Darboux transformation construction (2.8)–(2.9),

$$A_1 = \Psi(x,t,\lambda_1)\partial_x \frac{1}{\Psi(x,t,\lambda_1)} = \partial_x - V_1(x,t),$$
$$V_1(x,t) = (\log \Psi(x,t,\lambda_1))_x. \quad (2.12)$$

The operator A_1 and its Hermitian conjugate, $A_1^\dagger$, intertwine the Schrödinger operators $L = -\partial_x^2 + u(x,t)$ and $L_1 = -\partial_x^2 + u_1(x,t)$,

$$A_1 L = L_1 A_1, \qquad A_1^\dagger L_1 = L A_1^\dagger, \quad (2.13)$$

and factorize them,

$$A_1^\dagger A_1 = L - \lambda_1, \qquad A_1 A_1^\dagger = L_1 - \lambda_1. \quad (2.14)$$

The two relations in Eq. (2.14) are equivalent to Riccati equations for the function V_1,

$$V_1^2 + V_{1x} = u - \lambda_1, \qquad V_1^2 - V_{1x} = u_1 - \lambda_1. \quad (2.15)$$

For the successive Crum-Darboux transformations of orders $m-1$ and m, the corresponding Schrödinger operators L_{m-1} and L_m are related by means of the first-order differential operator

$$A_m = (\mathbb{A}_{m-1}\Psi(x,t,\lambda_m))\partial_x \frac{1}{(\mathbb{A}_{m-1}\Psi(x,t,\lambda_m))}$$
$$= \partial_x - V_m(x,t),$$
$$m = 1, ..., \quad (2.16)$$

and its conjugate, where $\mathbb{A}_n = A_n A_{n-1}...A_1$, $A_0 \equiv 1$. Then, as a generalization of Eqs. (2.13) and (2.14), we have $A_m L_{m-1} = L_m A_m$, $A_m^\dagger L_m = L_{m-1}A_m^\dagger$, and $A_m^\dagger A_m = L_{m-1} - \lambda_m$, $A_m A_m^\dagger = L_m - \lambda_m$, where $L_0 \equiv L$.

The superpotential V_m can be presented in terms of the Wronskians [25],

$$V_m(x,t) = \Omega_{m-1}(x,t) - \Omega_m(x,t),$$
$$\Omega_m = -(\log W(\Psi(x,t,\lambda_1), ..., \Psi(x,t,\lambda_m)))_x, \quad (2.17)$$

where we assume $\Omega_0 = 0$ and $W(\Psi(x,t,\lambda_1)) = \Psi(x,t,\lambda_1)$. It satisfies the Riccati equations

$$V_m^2(x,t) + (V_m(x,t))_x = u_{m-1}(x,t) - \lambda_m,$$
$$V_m^2(x,t) - (V_m(x,t))_x = u_m(x,t) - \lambda_m. \quad (2.18)$$

C. Multisoliton solutions of the KdV equation

The described picture with Darboux-Crum transformations can be illustrated by the construction of multisoliton solutions for the KdV equation.

The trivial solution of the KdV equation is $u_0 = 0$. In this case $L_0 = -\frac{\partial^2}{\partial x^2}$ corresponds to the Schrödinger operator for a free-particle system, and the evolution operator (2.4) reduces to $P_0 = -4\frac{\partial^3}{\partial x^3}$. The system (2.1) then takes the form

$$-\frac{\partial^2 \Psi}{\partial x^2} = \lambda \Psi, \qquad \frac{\partial \Psi}{\partial t} = -4\frac{\partial^3 \Psi}{\partial x^3}. \quad (2.19)$$

Acting on both sides of the first equation by $4\partial_x$ and summing up the result with the second equation, we obtain $\partial_t \Psi = 4\lambda \partial_x \Psi$. Therefore, $\Psi(x,t,\lambda) = \Psi(x + 4\lambda t, \lambda)$. For $\lambda = 0$, $\lambda = -\kappa^2 < 0$, and $\lambda = \kappa^2 > 0$, the pairs of linearly independent solutions of the system (2.19) can be chosen in the form

$$\Psi(x,t,\lambda = 0) = \{1, x\}, \quad (2.20)$$

$$\Psi(x,t,\lambda = -\kappa^2) = \{\cosh X^-, \sinh X^-\},$$
$$\Psi(x,t,\lambda = \kappa^2) = \{\cos X^+, \sin X^+\}, \quad (2.21)$$

where $X^\mp = \kappa(x - x_0 \mp 4\kappa^2 t)$. To apply the Darboux-Crum transformation to a trivial solution $u_0 = 0$, we have

different possibilities for choosing wave functions from the sets (2.20) and (2.21). The choice $\Psi(x, t, 0) = x$ gives rise by means of the first-order Darboux transformation (2.8) to the simplest but singular, time-independent solution of the KdV equation, $u_1(x) = 2/x^2$. The *nonsingular* solutions for the KdV equation are generated by choosing appropriately the eigenstates with eigenvalues $\lambda < 0$,

$$u_n(x, t) = -2\frac{\partial^2}{\partial x^2}\log W(\cosh X_1^-, \sinh X_2^-..., f(X_n^-)),$$

$$X_j^- = \kappa_j(x - x_{0j} - 4\kappa_j^2 t),\qquad (2.22)$$

where the last argument in the Wronskian is $f(X_n^-) = \sinh X_n^-$ if n is even, $n = 2l$, and $f(X_n^-) = \cosh X_n^-$ for odd $n = 2l + 1$; x_{0j} are the translation (phase) parameters, and the scale parameters κ_j have to obey the inequalities $0 < \kappa_1 < \kappa_2 < \kappa_3 < \ldots < \kappa_n$. The functions (2.22) correspond to n-soliton solutions of the KdV equation. The case $n = 2$ is illustrated in Fig. 1. When solitons in the solution (2.22) are well separated, the propagation to the right of the jth soliton can be characterized by the speed $\mathcal{V}_j = 4\kappa_j^2$ and amplitude $2\kappa_j^2$.
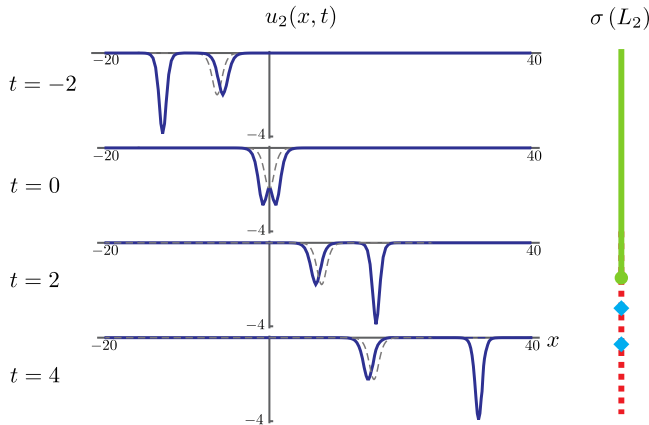

FIG. 1 (color online). The KdV two-soliton solution with $\kappa_1 = 1$, $\kappa_2 = 1.4$, and $x_{0i} = 0$, $i = 1, 2$ is shown by a continuous line. The propagation of a one-soliton solution with $\kappa_1 = 1$ and $x_{01} = 0$ is depicted by a dashed line. The initial phases are chosen so that the two-soliton and one-soliton solutions at $t = 0$ are symmetric with respect to the point $x = 0$. On the right, the spectrum of the associated two-soliton Schrödinger operator L_2 is shown. The continuous green line corresponds to a doubly degenerate semi-infinite continuous part of the spectrum with eigenstates $\psi^{\pm\kappa}(x, t) = \mathbb{A}_2 e^{\pm iX^+(x,t;\kappa,x_0)}$, while the filled circle indicates a nondegenerate edge state described by the eigenfunction $\psi_0(x, t) = \mathbb{A}_2 1$. The dashed red line corresponds to the nonphysical semi-infinite part of the spectrum, inside which blue squares indicate energies of the two bound states trapped by solitons and described by the eigenfunctions $\psi_1(x, t) = \mathbb{A}_2 \sinh X_1^-$ and $\psi_2(x, t) = \mathbb{A}_2 \cosh X_2^-$.

III. SPECTRAL PROBLEM WITH THE CNOIDAL BACKGROUND

The simplest stationary periodic solution to the KdV equation (2.5) can be presented in the form

$$u(x) = u_{0,0}(x) = 2k^2\mu^2\mathrm{sn}^2(\mu x|k) - \frac{2}{3}(1 + k^2)\mu^2, \quad (3.1)$$

where $\mathrm{sn}(u|k)$ is the Jacobi elliptic function, whose real and imaginary periods depend on the modular parameter $0 < k < 1$, $\mu > 0$ is a free (scale) parameter, and the sense of the indices in $u_{0,0}$ will be clarified below. Due to the t independence of the solution (3.1), the Lax equation (2.2) reduces to the condition of commutativity of the corresponding operators (2.3) and (2.4) constructed on the basis of Eq. (3.1),

$$[L, P] = 0. \qquad (3.2)$$

Equation (3.2) guarantees the existence of the common basis for the operators L and P. We then look for the solutions of the system of equations (2.6)–(2.7) in the form

$$\Psi(x, t, \lambda) = \Phi(x, \alpha)\exp(\pi(\alpha)t), \qquad (3.3)$$

where $\Phi(x, \alpha)$ is a common eigenstate of L and P, $L\Phi(x, \alpha) = \lambda(\alpha)\Phi(x, \alpha)$, $P\Phi(x, \alpha) = \pi(\alpha)\Phi(x, \alpha)$. The sought-for state $\Phi(x, \alpha)$ is [12,16,26]

$$\Phi(x, \alpha) = \frac{\mathrm{H}(\mu x + \alpha|k)}{\Theta(\mu x|k)}e^{-\mu x Z(\alpha|k)}, \qquad (3.4)$$

where H, Θ, and Z are Jacobi's eta, theta and zeta functions, while the corresponding eigenvalues are

$$\lambda(\alpha|k) = \mu^2\left(\mathrm{dn}^2(\alpha|k) - \frac{1}{3}(1 + k'^2)\right), \qquad (3.5)$$

$$\pi(\alpha|k) = -4k^2\mu^3\mathrm{sn}(\alpha|k)\mathrm{cn}(\alpha|k)\mathrm{dn}(\alpha|k). \qquad (3.6)$$

Notice that $\lambda(-\alpha) = \lambda(\alpha)$, $\pi(-\alpha) = -\pi(\alpha)$, $\pi(\alpha) = 2\mu\frac{d\lambda(\alpha)}{d\alpha}$, and

$$\pi^2(\alpha) = -16(\lambda(\alpha) - E_0)(\lambda(\alpha) - E_1)(\lambda(\alpha) - E_2), \quad (3.7)$$

where

$$E_0 = -\frac{1}{3}(1 + k'^2)\mu^2,$$

$$E_1 = \frac{1}{3}(1 - 2k^2)\mu^2,$$

$$E_2 = \frac{1}{3}(1 + k^2)\mu^2, \qquad (3.8)$$

and $k' = \sqrt{1 - k^2}$ is the complementary modular parameter. Equations (3.2) and (3.7) correspond to the

Burchnall-Chaundy theorem [27], and reflect the one-gap nature of the potential (3.1) [2,11] (see below).

Taking into account the double periodicity of the Jacobi sn, cn, and dn functions, without loss of generality one can suppose that a dimensionless parameter α takes values in the rectangle in the complex plane with vertices at[1] 0, $\mathbf{K}$, $\mathbf{K} + i\mathbf{K}'$, and $i\mathbf{K}'$. On the border of this *fundamental α rectangle*, eigenvalues $\lambda(\alpha)$ of the Schrödinger operator L take real values, while the eigenvalue $\pi(\alpha)$ of the Lax operator P takes nonzero real values on the horizontal borders of this rectangle where $\alpha = \beta^+$, $0 < \beta^+ < \mathbf{K}$, and $\alpha = \beta^- + i\mathbf{K}'$, $0 < \beta^- < \mathbf{K}$. On the other hand, on both vertical borders of the rectangle, $\alpha = i\gamma^+$, $0 \leq \gamma^+ < \mathbf{K}'$, and $\alpha = \mathbf{K} + i\gamma^-$, $0 \leq \gamma^- \leq \mathbf{K}'$, $\pi(\alpha)$ takes pure imaginary values, turning into zero at the vertices 0, $\mathbf{K}$, and $\mathbf{K} + i\mathbf{K}'$. The vertex $i\mathbf{K}'$ is the third-order pole of $\pi(\alpha)$ and the second-order pole of the function $\lambda(\alpha)$. Moreover, the corresponding eigenfunctions (3.4) are unbounded functions on the horizontal edges, but they are bounded on the vertical borders of the rectangle. Summarizing, in correspondence with the specified properties, the solutions (3.3) of the auxiliary spectral problem for the KdV equation are bounded on the vertical borders of the rectangle, except for the vertex point $\alpha = i\mathbf{K}'$, and they are unbounded on the horizontal borders except for the vertices $\alpha = 0$, $\mathbf{K}$, $\mathbf{K} + i\mathbf{K}'$.

The Schrödinger operator L with the potential (3.1) describes a quantum-mechanical periodic one-gap Lamé system, for which the upper horizontal line $\alpha = \beta^- + i\mathbf{K}'$ corresponds to the semi-infinite forbidden band with energy values $-\infty < E(\alpha) = \lambda(\alpha) < E_0$, and the lower horizontal line $\alpha = \beta^+$ corresponds to a spectral gap with $E_1 < E(\alpha) < E_2$. The corresponding bounds E_0, E_1, and E_2 defined in Eq. (3.8) satisfy the relations $E_0 < 0$, $E_2 > 0$, while E_1 can take positive or negative values depending on the value of the modular parameter k. The vertical borders of the rectangle correspond to the allowed valence [$\alpha = \mathbf{K} + i\gamma^-$, $E_0 \leq E(\alpha) \leq E_1$] and conduction [$\alpha = i\gamma^+$, $E_2 \leq E(\alpha) < \infty$] bands. By taking into account the relations $\lambda(-\alpha) = \lambda(\alpha)$, $\pi(-\alpha) = -\pi(\alpha)$, the common eigenstates of L and P with opposite values for $\pi(\alpha)$ are obtained from the described solutions with α restricted to the borders of the indicated rectangle by changing $\alpha \to -\alpha$.

Let us stress that the solutions (3.3) to the system of equations (2.6) and (2.7) have a factorizable dependence on the evolution variable t due to the t independence of the corresponding KdV solution (3.1) and the associated Lax pair (2.3)–(2.4).

IV. MULTISOLITON DEFECTS IN THE CRYSTALLINE BACKGROUND

One can construct three types of Darboux-Crum transformations based on the solutions (3.3) to the auxiliary

---

[1]Here, $\mathbf{K} = \mathbf{K}(k)$ is a complete elliptic integral of the first kind and $\mathbf{K}' = \mathbf{K}(k')$.

problem for the KdV equation. They will provide us with new soliton solutions of the KdV equation that propagate over the stationary crystalline background (3.1) by deforming it. These are

(i) soliton defects of the potential-well (pulse) type,
(ii) soliton defects of the compression modulation type, and
(iii) the mixed case in which both types of solitons are present.

Soliton defects of type i) are generated by Darboux-Crum transformations based on unbounded (nonphysical) states from the lower semi-infinite forbidden band in the spectrum of the one-gap Lamé system. The construction of soliton defects of type ii) requires the use of states from the gap of the quantum Lamé system. The employment of both types of nonphysical states from the spectrum of the Lamé system generates solutions corresponding to the mixed case iii). Below we describe these three types of solutions.

A. Potential-well (pulse) type solitons

If we choose the common eigenstates (3.3) of L and P in the form of real-valued functions, then the new solutions generated by the Darboux-Crum transformations (2.10) will also be real. The eigenfunctions $\Phi(x, \alpha = \beta^- + i\mathbf{K}')$, $\beta^- \in (0, \mathbf{K})$ of L in Eq. (3.4) correspond to nonphysical (unbounded) states with negative energies from the lower forbidden band of the one-gap Lamé system. They are real-valued functions modulo a global phase factor [12,16]. Omitting a phase factor, we obtain common real-valued eigenstates of L and P,

$$F(x, t, \beta^-) = \frac{\Theta(\mu x + \beta^- | k)}{\Theta(\mu x | k)} \exp(-\mu x \mathrm{z}(\beta^- | k) + \pi(\beta^- + i\mathbf{K}' | k)t), \tag{4.1}$$

where

$$\mathrm{z}(\beta^- | k) = \mathrm{Z}(\beta^- + i\mathbf{K}' | k) + i\frac{\pi}{2\mathbf{K}}$$
$$= \mathrm{Z}(\beta^- | k) + \frac{\mathrm{cn}(\beta^- | k)\mathrm{dn}(\beta^- | k)}{\mathrm{sn}(\beta^- | k)} > 0, \tag{4.2}$$

$$\pi(\beta^- + i\mathbf{K}' | k) = 4\mu^3 \frac{\mathrm{cn}(\beta^- | k)\mathrm{dn}(\beta^- | k)}{\mathrm{sn}^3(\beta^- | k)} > 0. \tag{4.3}$$

The superpotential (1.3) is given in terms of Eq. (4.1) by $V^{\mathrm{KA}}(x) = (\log F(x, t, \beta))_x$ with $\beta = \beta^-$ and $\mu = 1$, which reduces to Eq. (1.2) in the limit case $\beta^- = \mathbf{K}$. On the basis of the functions (4.1), we construct a Darboux-Crum transformation of the form

$$u_{0,l}(x,t) = u_{0,0}(x)$$
$$- 2(\log W(\mathcal{F}_+(1), \mathcal{F}_-(2), ..., \mathcal{F}_{(-1)^{l+1}}(l)))_{xx},$$
$$(4.4)$$

where

$$\mathcal{F}_\pm(j) = C_j^- F(x,t,\beta_j^-) \pm \frac{1}{C_j^-} F(x,t,-\beta_j^-),$$

$$j = 1, ..., l \qquad (4.5)$$

are combinations of the two linear independent solutions (4.1). The minus index in the parameter coefficients C_j^- indicates that Eq. (4.1) are real eigenstates from the *lower* forbidden band of the one-gap Lamé system. The choice

$$\mathbf{K} > \beta_1^- > \beta_2^- > \cdots > \beta_l^- > 0, \qquad 0 < C_j^- < \infty \qquad (4.6)$$

guarantees the nonsingular nature of the solution $u_{0,l}(x,t)$ for the KdV equation [12]. This solution describes l solitons of the potential-well type that propagate *to the right* in the stationary periodic background by deforming it. For large negative and positive values of t, pulses are well separated, and each corresponding potential well supports a bound state with negative energy given by Eq. (3.5) with $\alpha = \alpha_j = \beta_j^- + i\mathbf{K}'$. A deeper potential-well soliton defect in an asymptotically periodic background propagates faster, and supports the bound state with lower energy; see
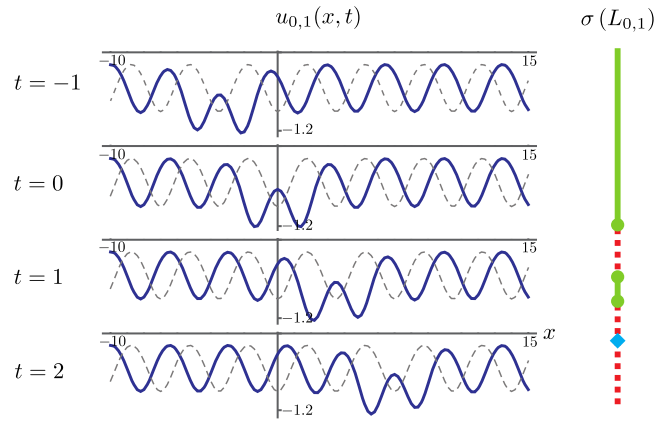

FIG. 2 (color online). The KdV solution with a pulse soliton propagating over the stationary crystalline background (3.1) shown by dashed line. Here $\mu = 1$, $k = 0.6$, $\beta_1^- = 1.2$, $C_1^- = 1$. The vertical line on the right illustrates the spectrum of the perturbed Lamé system with lower and upper forbidden bands shown in dashed red. The filled semicircles indicate nondegenerate energy values at the edges of the valence and conduction bands. In the semi-infinite lower forbidden band, there is a bound state trapped by the soliton defect, which is shown by a blue square. The parameters in Eq. (4.5) are chosen so that the solution at $t = 0$ is symmetric under the space reflection $x \to -x$.
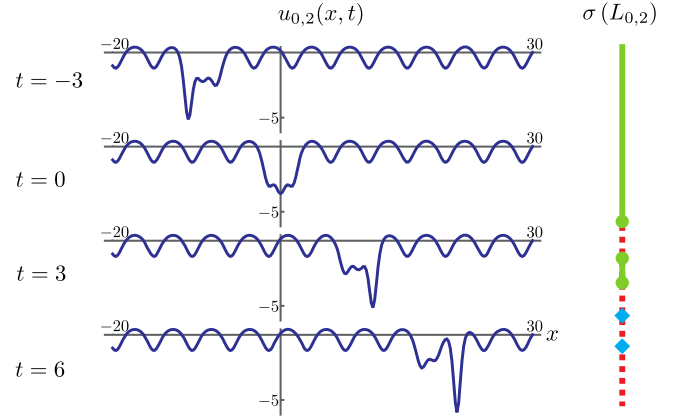

FIG. 3 (color online). A pair of pulse solitons in the asymptotically periodic background of the KdV solution. Here $\mu = 1$, $k = 0.9$, $\beta_1^- = 0.8$, $\beta_2^- = 0.6$, $C_1^- = C_2^- = 1$. As in the case of the asymptotically free background shown in Fig. 1, a deeper defect propagates with a higher speed. Each of the two defects here supports a bound state in the lower forbidden semi-infinite band of the perturbed one-gap Lamé system.

Sec. IV D. Figures 2 and 3 show such travelling soliton defects for the simplest cases of $l = 1$ and $l = 2$. In described solutions, an arbitrary number of solitons can be eliminated by taking limits of the type $C_j^- \to 0$ or $C_j^- \to \infty$ which correspond to sending the jth soliton to minus or plus infinity. This provokes a global phase shift $x \to x - \frac{\mu}{\beta_j^-}$ for $C_j^- \to 0$, or $x \to x + \frac{\mu}{\beta_j^-}$ when $C_j^- \to \infty$, in the crystalline background as well as in the remaining solitons, and an additional change in the parameters $C_{j'}^-$, $j' \neq j$, which depend on $\beta_{j'}^-$ and β_j^-; see Refs. [12,28].

The indicated phase shifts of the crystalline background can be understood in the following simple way. Consider the first-order Darboux transformation based on the function $F(x, \beta^-)$ from Eq. (4.1) and applied to the stationary periodic KdV solution (3.1). Since $\log F(x, \beta^-) = \log \Theta(\mu x + \beta^-|k) - \log \Theta(\mu x|k) - (\mu x \mathbf{z}(\beta^-|k) - \pi(\beta^- + i\mathbf{K}'|k)t)$, and $-2(\log \Theta(\mu x|k))_{xx} = u_{0,0}(x)$, we see that the Darboux transformation generated by $F(x, \beta^-)$ transforms $u_{0,0}(x)$ into $u_{0,0}(x + \beta^-/\mu)$, while the transformation based on $F(x, -\beta^-)$ produces the displacement $x \to x - \beta^-/\mu$. When we take the limit $C_j^- \to 0$ in the Darboux-Crum transformation (4.4), in the function (4.5) the term with $F(x, -\beta_j^-)$ survives. Due to the relation $\mathbf{z}(-\beta_j^-|k) < 0$, this function exponentially increases in the region $x \to +\infty$, and this provokes the displacement $x \to x - \beta^-/\mu$ of the asymptotically periodic background of the solution in that region. Analogously, for the limit $C_j^- \to \infty$, the first term with $F(x, \beta_j^-)$ survives in the function (4.5), and the asymptotically periodic background in the solution will be displaced by the shift $x \to x + \beta^-/\mu$ in the region to the left ($x \to -\infty$) of the rest of the surviving solitons.

B. Solitons of the compression modulation type

The states (3.3) with $\alpha = \pm\beta^+$, $0 < \beta^+ < \mathbf{K}$, which we denote here as $\Phi(x, t, \pm\beta^+)$,

$$\Phi(x, t, \beta^+) = \frac{\mathrm{H}(\mu x + \beta^+|k)}{\Theta(\mu x|k)} \exp(-\mu x Z(\beta^+|k) + \pi(\beta^+|k)t),$$ (4.7)

where $Z(\beta^+|k) > 0$ and

$$\pi(\beta^+|k) = -4\mu^3 k^2 \mathrm{sn}(\beta^+|k)\mathrm{cn}(\beta^+|k)\mathrm{dn}(\beta^+|k) < 0,$$ (4.8)

correspond to the energy gap (finite, upper forbidden band) $E_1 < E(\alpha) < E_2$ [see Eq. (3.8)] in the spectrum of the Lamé system. They are represented by real functions, and can be used in the Darboux transformation (2.8). These functions, however, have an infinite number of zeros on the real line, and their use would produce a singular transformation. To resolve this problem, in the simplest case we can realize a second-order $(n = 2)$ Darboux-Crum transformation (2.10), $u_{2,0}(x,t) = u_{0,0}(x) - 2(\log W(\Phi_+(1), \Phi_-(2)))_{xx}$, by taking $\Phi_+(1) = C_1^+ \Phi(x, t, \beta_1^+) + \frac{1}{C_1^+}\Phi(x, t, -\beta_1^+)$ and $\Phi_-(2) = C_2^+ \Phi(x, t, \beta_l^+) - \frac{1}{C_2^+}\Phi(x, t, -\beta_2^+)$, with $0 < \beta_1^+ < \beta_2^+ < \mathbf{K}$ and $C_{1,2}^+ > 0$. The nonsingular potential $u_{2,0}(x, t)$ supports two bound states in the spectrum of the Schrödinger operator L with energy values given by Eq. (3.5), which are in the gap, between the two continuous bands of the Lamé system. The solution $u_{2,0}(x, t)$ of the KdV equation, depicted in Fig. 4, describes the propagation of the two solitons of the compression modulation type in the asymptotically periodic background. They are similar to the so-called grey solitons;
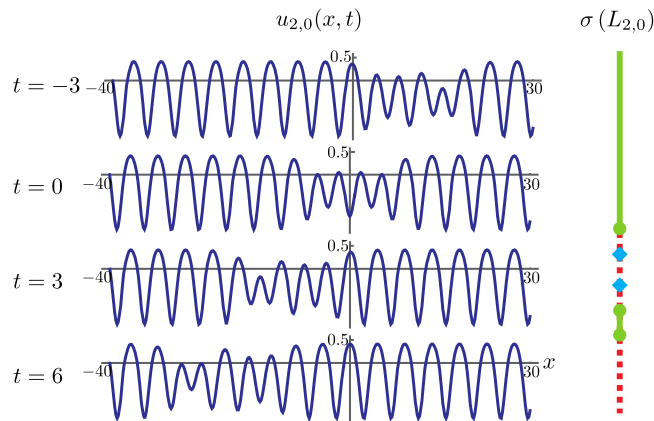

FIG. 4 (color online). A pair of solitons of the compression modulation type propagating to the left in a stationary crystalline background. Here $\mu = 1$, $k = 0.9$, $\beta_1^+ = 1$, $\beta_2^+ = 1.3$, $C_1^+ = C_2^+ = 1$. Due to the presence of the valence band in the spectrum of the Lamé system $L_{0,0}$, defects of this type have no direct analogs in the asymptotically free, homogeneous background case.

see Refs. [5,29,30]. The described Darboux-Crum procedure can be generalized to obtain the potential supporting the $2l$ bound states in the gap,

$$u_{2l,0}(x, t) = u_{0,0}(x) - 2(\log W(\Phi_+(1),$$
$$\Phi_-(2), ..., \Phi_+(2l - 1), \Phi_-(2l)))_{xx},$$ (4.9)

$$\Phi_{(-1)^{j+1}}(j) = C_j^+ \Phi(x, t, \beta_j^+) + (-1)^{j+1}\frac{1}{C_j^+}\Phi(x, t, -\beta_j^+),$$

$$j = 1, ..., 2l,$$ (4.10)

$$0 < \beta_1^+ < \beta_2^+ < \cdots < \beta_l^+ < \mathbf{K}, \qquad 0 < C_j^+ < \infty.$$ (4.11)

The solution $u_{2l,0}(x, t)$ has $2l$ compression modulation type solitons which move *to the left* in the stationary crystalline background.

In the definition of the wave functions (4.5) and (4.10), which are linear combinations of the eigenstates of the Lax operator P with opposite eigenvalues $\pi(\alpha)$ and $-\pi(\alpha)$, the dependence on the evolution parameter t can be transferred from the common eigenstates of L and P into corresponding coefficients C_j^- and C_j^+. In this way, the function (4.10) can be presented equivalently in the form $\Phi_{(-1)^{j+1}}(j) = C_j^+(t)\Phi(x, t = 0, \beta_j^+) + (-1)^{j+1}\frac{1}{C_j^+(t)}\Phi(x, t = 0, -\beta_j^+)$, where $C_j^+(t) = C_j^+ \exp(\pi(\beta_j^+)t)$, and $\pi(\beta_j^+)$ is given by Eq. (4.8) with β^+ substituted for β_j^+. For Eq. (4.5) we have an analogous equivalent representation with $\pi(\beta^- + i\mathbf{K}')$ given by Eq. (4.3).

To obtain the solution with an odd number of solitons of the compression modulation type, there are the following possibilities. We can choose one of the arbitrary constants C_j^+ and apply to the solution (4.9) the limit $C_j^+ \to 0$ (or $C_j^+ \to \infty$). Such a limit results in sending the jth soliton to $x = -\infty$ (or $x = +\infty$) without affecting the rest of the solitons except for inducing a global phase shift in them and in the background (equal to $x \to x - \frac{\beta_j^+}{\mu}$ for $C_j^+ \to 0$ and $x \to x + \frac{\beta_j^+}{\mu}$ for $C_j^+ \to \infty$) due to the nonlinear interaction in the KdV equation, and an additional change in the constants $C_{j'}^+$, $j' \neq j$, depending on $\beta_{j'}^+$ and β_j^+; see Ref. [28]. Another option to generate the solution with an odd number of solitons of the compression modulation type is to take $\beta_1^+ = 0$ [in this case, $\Phi_+(1) \propto \mathrm{sn}(\mu x|k)$] or $\beta_{2l}^+ = \mathbf{K}$ [then, $\Phi_-(2l) \propto \mathrm{cn}(\mu x|k)$]. One of the indicated states corresponds to the edge of the conduction band of the one-gap Lamé system ($\beta_1^+ = 0$), while another one corresponds to the upper edge of the valence band ($\beta_{2l}^+ = \mathbf{K}$). The same effect can be obtained just by applying the limit $\beta_1^+ \to 0$, or $\beta_{2l}^+ \to \mathbf{K}$ in Eq. (4.9), which results in eliminating the corresponding bound state from the spectrum of

the Schrödinger system $L = -\frac{d^2}{dx^2} + u_{2l,0}(x,t)$; see Ref. [12]. The issue of the velocities for the described solutions will be discussed below, in Sec. IV D.

C. Mixed case

In the mixed case, the Darboux-Crum transformation takes the form

$$u_{2l,m}(x,t) = u_{0,0}(x) - 2(\log W(\Phi_+(1), \Phi_-(2), \ldots, \Phi_-(2l),$$
$$\mathcal{F}_+(1), \mathcal{F}_-(2), \ldots, \mathcal{F}_{(-1)^m}(j)))_{xx}. \quad (4.12)$$

This solution has $2l$ solitons of the compression modulation type, which move to the left, and m solitons of the potential-well type, which propagate to the right. In the associated Schrödinger system $L_{2l,m} = -\frac{d^2}{dx^2} + u_{2l,m}(x,t)$, the potential-well and compression modulation type solitons support the bound states in the lower forbidden band and in the gap of the energy spectrum, respectively. In Fig. 5, one can see how solitons of different types propagate in opposite directions over the stationary background.

Here, the case with an odd number of the solitons of the compression modulation type can be obtained from Eq. (4.12) in the way described in Sec. IV B.
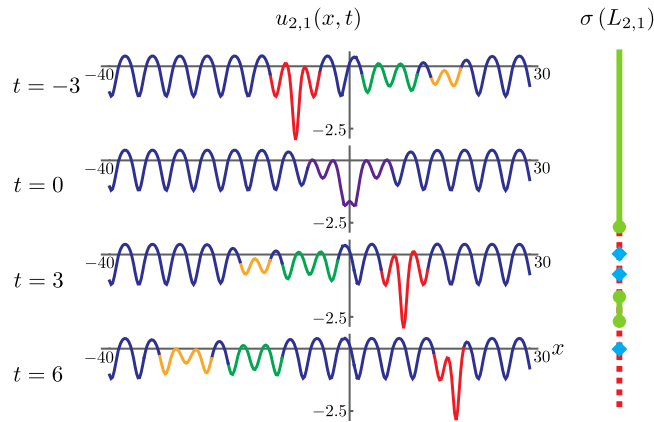

FIG. 5 (color online).   The KdV solution with one pulse soliton (given by β_1^- and shown in red) propagating to the right, and two solitons of the compression modulation type (characterized by β_1^+ and β_2^+ and depicted in orange and green, respectively) moving to the left in a stationary crystalline background. The more rapid compression soliton (β_1^+) supports a bound state of higher energy in the spectrum of the associated Schrödinger system $L_{2,1} = -\frac{d^2}{dx^2} + u_{2,1}(x,t)$. At the moment $t = 0$, solitons are in the zone of a strong interaction, shown in violet, and are not well separated. The color highlighting used here is rather conditional since the defects are transformed into a background asymptotically. The parameters are chosen so that the solution at $t = 0$ is symmetric with respect to the point $x = 0$. Here, $\mu = 1$, $k = 0.9$, $\beta_1^- = 0.9$, $\beta_1^+ = 1$, $\beta_2^+ = 1.3$, $C_1^- = C_{1,2}^+ = 1$.

D. On velocities and amplitudes of solitons in crystalline background

For the asymptotically free solutions discussed in Sec. II C, the multisoliton solution can be presented in the form (2.22), which is similar to the form of the second term on the right in Eqs. (4.4), (4.9), or (4.12). The hyperbolic cosh and sinh functions in Eq. (2.22) are just the linear combinations of the exponents $\exp(\kappa_j(x - 4\kappa_j^2 t))$ and $\exp(-\kappa_j(x - 4\kappa_j^2 t))$ with constant coefficients. As a result, when solitons are well separated (this happens for sufficiently large values of $|t|$), the solution (2.22) reduces to the sum of one-soliton solutions, $u_n(x,t) \approx \sum_{j=1}^n -2\kappa_j^2 \text{sech}^2(\kappa_j(x - \tilde{x}_{0j} - 4\kappa_j^2 t))$, with obviously identified velocities and amplitudes. Since the exponents in Eqs. (4.1) and (4.7) are odd functions of the parameters β^- and β^+, respectively, Eqs. (4.5) and (4.10) (similarly to the hyperbolic functions) are linear combinations of the exponents with arguments of the form $\varphi(x - \mathcal{V}t)$ and $-\varphi(x - \mathcal{V}t)$, but now with coefficients that are certain periodic functions of x. As a consequence (unlike the case of the KdV solutions over the asymptotically free background), how to define the amplitudes and velocities of solitons propagating in the crystalline background is not so obvious. Even when defects are well separated, their velocities and amplitudes are varied at each instant of time due to their nonlinear, position-dependent interaction with the oscillating background. Nevertheless, by analogy with the asymptotically free case, one can observe that the quantities $\mu^2 z^2(\beta^-|k)$ and $\mu^2 Z^2(\beta^+|k)$ give us relevant information on the amplitudes of the well-separated pulse and modulation type defects, respectively, provided that for a well-separated soliton defect the corresponding preexponential periodic factor in Eq. (4.1) or Eq. (4.7) associated with the crystalline background will be less significant than the exponential factors there. This observation implies a monotonic increase of the amplitude of the pulse type soliton with an increase of the energy modulus of the bound state trapped by it in the spectrum of the associated perturbed one-gap Lamé system. Such a monotonic increase will be valid, however, starting from some sufficiently low energy value inside the lower forbidden band of the spectrum. For soliton defects of the compression modulation type the picture is more complicated, since in the interval $0 < \beta^+ < \mathbf{K}$ the function $Z^2(\beta^+|k)$ takes a zero value when β^+ tends to zero, then monotonically increases until some maximum value at some β_*^+ inside the indicated interval, and finally monotonically decreases, taking a zero value at the edge $\beta^+ = \mathbf{K}$. So, we can only conclude that the amplitude of the compression modulation type defect will tend to zero when the energy of the bound state trapped by it approximates the edges of the gap in the spectrum of the perturbed one-gap Lamé system, and will take some maximal value at some energy of the corresponding trapped bound state inside the gap. With the same

reservations one can say that the width of the defects is proportional to $1/\mu z(\beta^-)$ and $1/\mu Z(\beta^+)$ for the pulse and modulation type solitons, respectively.

To define the velocities of the solitons, we consider the case of a well-separated defect of the pulse type, while for the compression modulation type defect the reasoning will be similar.

The well-separated pulse soliton with index j will have the form described by the one-soliton solution $u_{0,1}$ given by Eq. (4.4) with some parameter C_1^- and $\beta_1^- = \beta_j^-$, i.e., this soliton will depend only on the eigenstate $\mathcal{F}_+(j)$ with a certain parameter C_j^-. Then we can identify the velocity of this soliton from the condition that $u_{0,1}(x, t) = u_{0,1}(x + \Delta_x, t + \Delta_t)$ is valid for all x and t for which the soliton remains well separated from other defects, where Δ_x and Δ_t are some constants. This condition has a solution with $\Delta_x = nT$, where $T = \frac{2\mathbf{K}}{\mu}$ corresponds to the period of the asymptotically periodic crystalline background and $\Delta_t = n2\mathbf{K}z(\beta_j^-|k)/(\mu\pi(\beta_j^- + i\mathbf{K}'|k))$, while n is any integer not violating the condition of separation of the soliton. From here we identify the velocity of the pulse soliton as $\mathcal{V}(\beta_j^-) = \Delta_x/\Delta_t$, and obtain

$$\mathcal{V}(\beta_j^-) = \frac{4\mu^2 \frac{\mathrm{cn}(\beta_j^-|k)\mathrm{dn}(\beta_j^-|k)}{\mathrm{sn}^3(\beta_j^-|k)}}{\mathrm{Z}(\beta_j^-|k) + \frac{\mathrm{cn}(\beta_j^-|k)\mathrm{dn}(\beta_j^-|k)}{\mathrm{sn}(\beta_j^-|k)}} > 0. \quad (4.13)$$

This corresponds to the velocity with which a fixed value of the argument of the exponent in Eq. (4.1) propagates in space and time, $\varphi(x - \mathcal{V}t) = \mathrm{const}.$

In a similar way, for the compression modulation type defect we find

$$\mathcal{V}(\beta_j^+) = -4\mu^2 k^2 \frac{\mathrm{sn}(\beta_j^+|k)\mathrm{cn}(\beta_j^+|k)\mathrm{dn}(\beta_j^+|k)}{\mathrm{Z}(\beta_j^+|k)} < 0. \quad (4.14)$$

For $\beta_j^- \to 0$, the energy of the bound state trapped by the pulse defect tends to minus infinity, and the amplitude and velocity (4.13) of the soliton tend to infinity, while its width tends to zero. For $\beta_j^- \to \mathbf{K}$, the amplitude of the soliton tends to zero, its width tends to infinity, and the limit of Eq. (4.13) is finite and equals

$$\lim_{\beta_j^- \to \mathbf{K}} \mathcal{V}(\beta_j^-) = 4\mu^2 k'^2 \frac{\mathbf{K}}{\mathbf{E}}. \quad (4.15)$$

Here $\mathbf{E}$ is the complete elliptic integral of the second kind, and as a consequence of the inequality relations $\frac{1}{k'^2} > \frac{\mathbf{K}}{\mathbf{E}} > 1$ [16] one finds that the limit value (4.15) is inside the interval $(4\mu^2 k'^2, 4\mu^2)$.

Similarly, for the compression modulation type defect, in the limits when its amplitude tends to zero its velocity tends to nonzero limits,

$$\lim_{\beta_j^+ \to 0} \mathcal{V}(\beta_j^+) = -4\mu^2 k^2 \frac{\mathbf{K}}{\mathbf{K} - \mathbf{E}} < 0,$$

$$\lim_{\beta_j^+ \to \mathbf{K}} \mathcal{V}(\beta_j^+) = -4\mu^2 k^2 k'^2 \frac{\mathbf{K}}{\mathbf{E} - k'^2\mathbf{K}} < 0, \quad (4.16)$$

while its width tends to infinity.

E. Galilean symmetry

The described solutions can be modified by employing the Galilean symmetry of the KdV equation. This symmetry means that if $u(x, t)$ is a solution of the KdV equation $u_t = 6uu_x - u_{xxx}$, then $u_G(x, t) = u(x - 6Gt, t) - G$ is also a solution of the KdV equation for any choice of a real constant G. In the described solutions, the crystalline background over which the soliton defects propagate (deforming it due to a nonlinear interaction) was static. The application of Galilean transformations to the solutions will boost the defects and background and also vertically shift the solutions by the additive constant $-G$. However, this Galilean transformation will not change the relative velocities between defects and their velocities with respect to the boosted crystalline background. As we shall see below, the Galilean symmetry of the KdV equation will play a crucial role in the construction of the solutions for the mKdV equation by means of the Miura-Darboux-Crum transformations.

V. UNIFICATION OF THE KdV AND mKdV EQUATIONS BY MIURA-DARBOUX-CRUM TRANSFORMATIONS, AND EXOTIC SUPERSYMMETRY

A. Miura-Darboux-Crum transformations

The defocusing mKdV equation and the KdV equation,

$$v_t - 6v^2 v_x + v_{xxx} = 0,$$
$$u_t - 6uu_x + u_{xxx} = 0, \quad (5.1)$$

are related by the Miura transformation [31]. Namely, the substitution of $u^{\pm} = v^2 \pm v_x$ into the KdV equation gives

$$u_t^{\pm} - 6u^{\pm}u_x^{\pm} + u_{xxx}^{\pm} = (2v \pm \partial_x)(v_t - 6v^2 v_x + v_{xxx}). \quad (5.2)$$

The two relations in Eq. (5.2) mean that if v is a solution of the mKdV equation, then both $u^{\pm}$ satisfy the KdV equation. On the other hand, if both u^+ and u^- are solutions of the KdV equation, and there exists a v such that $u^{\pm} = v^2 \pm v_x$, then v obeys the mKdV equation [25]. Unlike the KdV case, if $v(x, t)$ is the mKdV solution, then $-v(x, t)$ is also a solution.

From the chains of the Darboux-Crum transformations we know that the function $V_m(x, t)$ in Eq. (2.17) and the corresponding solutions of the KdV equation $u_m(x, t)$ and $u_{m-1}(x, t)$ are related by

$$V_m^2(x,t) + (V_m(x,t))_x = u_{m-1}(x,t) - \lambda_m,$$
$$V_m^2(x,t) - (V_m(x,t))_x = u_m(x,t) - \lambda_m. \tag{5.3}$$

With taking into account the Galilean symmetry of the KdV equation, we displace $x \to x - 6\lambda_m t$, and make a change $u(x,t) \to u(x - 6\lambda t, t) - \lambda \equiv u^\lambda(x,t)$. Equation (5.3) will then transform into

$$v_m^2(x,t) + (v_m(x,t))_x = u_{m-1}^{\lambda_m}(x,t),$$
$$v_m^2(x,t) - (v_m(x,t))_x = u_m^{\lambda_m}(x,t), \tag{5.4}$$

where $v_m(x,t) = V_m(x - 6\lambda_m t, t)$. The $v_m(x,t)$ are therefore solutions of the mKdV equation.

Utilizing this observation and solutions of the KdV equation obtained by means of the Darboux-Crum transformations, we can construct an infinite number of solutions for the mKdV equation. The KdV solutions from Sec. II C will provide us with the mKdV solitons taking constant asymptotic values at infinity. On the basis of the KdV multisoliton defects from the preceding section, we will obtain solutions for the mKdV equation in the form of soliton defects propagating in the crystalline background.

B. Exotic $N = 4$ nonlinear supersymmetry

Before we proceed to the discussion of the solutions to the mKdV equation and their peculiarities, we note that on the basis of the relations (5.4) the corresponding solutions of the KdV and mKdV equations can be related using the exotic $N = 4$ nonlinear supersymmetry. Besides an ordinary $N = 2$ supersymmetry, it incorporates two nontrivial Lax-Novikov integrals for the two Schrödinger subsystems associated with the KdV equation, as well as two additional supercharges that are higher-order matrix differential operators.

To reveal the exotic supersymmetric structure, we first note that an ordinary $N = 2$ supersymmetry in the form of a superalgebra

$$[\mathcal{L}_m, \mathcal{S}_{m,a}] = 0, \qquad \{\mathcal{S}_{m,a}, \mathcal{S}_{m,b}\} = 2\mathcal{L}_m \delta_{ab},$$
$$a, b = 1, 2 \tag{5.5}$$

(with σ_3 identified as a $\mathbb{Z}_2$ grading operator) is generated by the extended, matrix Schrödinger Hamiltonian $\mathcal{L}_m$ and the associated Dirac Hamiltonian $\mathcal{D}_m$,

$$\mathcal{L}_m = \begin{pmatrix} L_{m-1}(m) & 0 \\ 0 & L_m(m) \end{pmatrix},$$
$$\mathcal{D}_m = \begin{pmatrix} 0 & A_m^\dagger(m) \\ A_m(m) & 0 \end{pmatrix}, \tag{5.6}$$

where $\mathcal{S}_{m,1} = \mathcal{D}_m$ and $\mathcal{S}_{m,2} = i\sigma_3 \mathcal{D}_m$. The Schrödinger operators $L_{m-1}(m)$ and $L_m(m)$, $L_n(m) = -\frac{d^2}{dx^2} + u_n^{\lambda_m}(x,t)$,

$n = m - 1$, m are related here by the Darboux (Miura) transformation generated by the first-order operators $A_m(m)$ and $A_m^\dagger(m)$, where $A_m(n) = \frac{d}{dx} - V_m(x - 6\lambda_n t, t)$, and the solution of the mKdV equation $v_m(x,t) = V_m(x - 6\lambda_m t, t)$ can be considered as a superpotential.

Let us recall that for the quantum-mechanical operators $\mathcal{L}_m$ and $\mathcal{D}_m$ the parameter t does not correspond to the Schrödinger or Dirac evolution; rather, it is associated here with the coherent peculiar isospectral deformations of their potentials governed by the KdV and mKdV equations. Any Schrödinger system with a multisoliton or finite-gap potential can be characterized by a nontrivial integral of motion in the form of the Lax-Novikov higher-derivative differential operator of odd order [2,11,27]. As a consequence, for the extended matrix system $\mathcal{L}_m$ composed offrom a pair of such peculiar Schrödinger subsystems related by a Darboux transform, the quantum-mechanical $N = 2$ supersymmetry associated with the fermionic integrals $\mathcal{S}_{m,a}$ is extended up to the exotic $N = 4$ nonlinear supersymmetry incorporating two additional supercharges $\mathcal{Q}_{m,a}$. Additional supercharges are composed from higher (even)-order differential operators which intertwine the diagonal elements in $\mathcal{L}_m$, and together with the building blocks of the supercharges $\mathcal{S}_{m,a}$ [which are the first-order differential operators $A_m(m)$ and $A_m^\dagger(m)$] effectively factorize the Lax-Novikov integrals of the extended Schrödinger system $\mathcal{L}_m$. For the discussion of a general structure of the exotic $N = 4$ nonlinear supersymmetry associated with finite-gap and soliton systems see Refs. [15,16,25,28,32,33] and references therein.

Specifically, here the extension of $N = 2$ supersymmetry up to the exotic $N = 4$ nonlinear supersymmetry happens as follows. We have started with the stationary solution (3.1) for the KdV equation to construct solutions $u_m(x,t)$. For the initial Schrödinger operator $L_0 = -\frac{d^2}{dx^2} + u_0(x)$, $u_0(x) = u_{0,0}(x)$, we can construct the first-order operator (2.12), $A_1(x,t) = \frac{d}{dx} - v_1(x,t)$, which provides us with the intertwining relation $A_1 L_0 = L_1 A_1$, where $L_1 = -\frac{d^2}{dx^2} + u_1(x,t)$. The Lax operator $P_0 = P(u_0)$ constructed on the basis of the stationary solution $u_0(x)$ satisfies Eq. (3.2), $[P_0, L_0] = 0$. Being the third-order differential operator, this is the Lax-Novikov integral for the Schrödinger system L_0. The intertwining relation $A_1 L_0 = L_1 A_1$ and the conjugate relation show that for the Schrödinger system L_1, the fifth-order differential operator $P_1(x,t) = A_1 P_0 A_1^\dagger$ is the Lax-Novikov integral of motion, $[P_1, L_1] = 0$. Then, by applying the Galilean transformation with the parameter $G = \lambda_1$ to the KdV solutions $u_0(x)$ and $u_1(x,t)$, we obtain the fifth-order operators $P_1(1) = A_1(1)P_0(x - 6\lambda_1 t)A_1^\dagger(1)$ and $P_0(1) = L_0(1)P_0(x - 6\lambda_1 t) = A_1^\dagger(1)A_1(1)P_0(x - 6\lambda_1 t)$, which are integrals for $L_1(1)$ and $L_0(1)$, respectively. Being the product of the integral $P_0(x - 6\lambda_1 t)$ with the Schrödinger Hamiltonian $L_0(1)$, in

this case the integral $P_0(1)$ is reducible. However, we use it to construct two bosonic integrals for the extended system $\mathcal{L}_1$,

$$\mathcal{P}_{1,1} = \begin{pmatrix} P_0(1) & 0 \\ 0 & P_1(1) \end{pmatrix}, \qquad \mathcal{P}_{1,2} = \sigma_3 \mathcal{P}_{1,1}, \quad (5.7)$$

where the matrix elements are differential operators of the same order.

To get the analogs of the integrals (5.7) for a general case corresponding to the extended Schrödinger system described by $\mathcal{L}_m$, we have to change the fifth-order differential operator $A_1 P_0 A_1^\dagger$ for $\mathbb{A}_m P_0 \mathbb{A}_m^\dagger$ which is a differential operator of order $2m + 3$ commuting with the Schrödinger operator $L_m = -\frac{d^2}{dx^2} + u_m(x, t)$. Then we realize a usual Galilean transformation with the velocity $-6\lambda_m$ to obtain the operator $P_m(m) = \mathbb{A}_m(m) P_0(x - 6\lambda_m t) \mathbb{A}_m^\dagger(m)$, which is the Lax-Novikov integral for the quantum system $L_m(m)$. In a similar way, as an analog of $L_0(1) P_0(x - 6\lambda_1 t)$ we get the operator $P_{m-1}(m) = L_{m-1}(m) \mathbb{A}_{m-1}(m) P_0(x - 6\lambda_m t) \mathbb{A}_{m-1}^\dagger(m)$ which commutes with $L_{m-1}(m)$, where $\mathbb{A}_n(m) = A_n(m) A_{n-1}(m) \ldots A_1(m)$. In this manner we obtain a pair of matrix operators $\mathcal{P}_{m,1} = \text{diag}(P_{m-1}(m), P_m(m))$ and $\mathcal{P}_{m,2} = \sigma_3 \mathcal{P}_{m,1}$, which are the integrals for the extended Schrödinger system $\mathcal{L}_m$, and in addition to Eq. (5.5) we get the relations

$$[\mathcal{P}_{m,a}, \mathcal{L}_m] = [\mathcal{P}_{m,a}, \mathcal{P}_{m,b}] = [\mathcal{P}_{m,1}, \mathcal{S}_{m,b}] = 0. \quad (5.8)$$

At the same time, the commutator of $\mathcal{P}_{m,2}$ with $\mathcal{S}_{m,a}$, $a = 1, 2$ will supply us with a pair of new fermionic integrals $\mathcal{Q}_{m,a}$, which are differential operators of even order $2m$ that also commute with $\mathcal{P}_{m,1}$, $[\mathcal{P}_{m,1}, \mathcal{Q}_{m,b}] = 0$. So, the operator $\mathcal{P}_{m,1}$, like $\mathcal{L}_m$, is the bosonic central charge of the superalgebra. Together, two bosonic integrals $\mathcal{P}_{m,a}$, $a = 1, 2$ allow us to distinguish the eigenstates corresponding to the fourfold degenerate eigenvalues inside the continuous allowed bands of $\mathcal{L}_m$. Also, they detect all the edge states and all the bound states in the spectrum of $\mathcal{L}_m$ by annihilating them. The fermionic integrals $\mathcal{S}_{m,a}$ and $\mathcal{Q}_{m,a}$ generate transformations between the "up" and "down" eigenstates of the same eigenvalues in the spectrum of $\mathcal{L}_m$, and as usual complex linear combinations of $\mathcal{S}_{m,1}$ and $\mathcal{S}_{m,2}$ and of $\mathcal{Q}_{m,1}$ and $\mathcal{Q}_{m,2}$ will be creation- and annihilation-type operators for those eigenstates. The bosonic integral $\mathcal{P}_{m,2}$ generates a kind of rotation between the supercharges $\mathcal{S}_a$ and $\mathcal{Q}_a$ [12,25,28].

The four fermionic supercharges $\mathcal{S}_{m,a}$ and $\mathcal{Q}_{m,a}$ and two bosonic integrals $\mathcal{P}_{m,a}$ together with the matrix Schrödinger Hamiltonian $\mathcal{L}_m$ generate the exotic nonlinear $N = 4$ supersymmetry, whose superalgebraic relations will contain coefficients that are polynomials in the central charge $\mathcal{L}_m$. Such an unusual nonlinear extension of supersymmetric structure related to integrable systems was discussed in different aspects in

Refs. [12,15,16,28,32,33]. The anticommutation relations for $\mathcal{S}_{m,a}$ in Eq. (5.5), and similar relations for $\mathcal{Q}_{m,a}$ where the right-hand side is a certain polynomial of order m in $\mathcal{L}_m$, together reflect the fact that the square of the Lax-Novikov integrals $\mathcal{P}_{m,a}$ (in correspondence with the Burchnall-Chaundy theorem [27]) is a certain polynomial of odd order $(2m + 1)$ in $\mathcal{L}_m$.

Systems also exist (explicit examples of which will be considered below) where the described structure of the exotic supersymmetry can be reduced in the order of the differential operators corresponding to the set of integrals $\mathcal{P}_a$ and $\mathcal{Q}_a$. This happens when the Schrödinger potentials $u_m^{\lambda_m}(x, t)$ and $u_{m-1}^{\lambda_m}(x, t)$ are completely isospectral, and the ordinary $N = 2$ supersymmetry generated by the first-order supercharges $\mathcal{S}_a$ in accordance with Eq. (5.5) is spontaneously broken. Specifically, in the case when the Schrödinger potentials $u_m^{\lambda_m}(x, t)$ and $u_{m-1}^{\lambda_m}(x, t)$ have a difference in one bound state in the spectra of the systems $L_m(m)$ and $L_{m-1}(m)$, the spectrum of the corresponding Dirac Hamiltonian with the scalar potential $v_m(x, t)$ will contain one kink as a defect. If this is the case, there is no reduction in the structure of the exotic supersymmetry generators; the envelope of the corresponding oscillating eigenfunction $\Psi_m(x)$ of the initial one-gap Lamé system used in the Darboux-Crum construction will exponentially increase in both the positive and negative x directions. In contrast, when the envelope of $\Psi_m(x)$ increases exponentially in one direction and decreases exponentially in the other direction, the corresponding first-order intertwining operator $A_m(m) = X_{m-1}(m) = \frac{d}{dx} - v_{m-1}(x, t, \lambda_m)$ generates a nonlinear shift in the already present soliton defects as well as in the background, without adding a bound state to the spectrum of $L_m(m) \equiv \tilde{L}_{m-1}(m)$ in comparison with that of $L_{m-1}(m)$, $X_{m-1}(m) L_{m-1}(m) = \tilde{L}_{m-1}(m) X_{m-1}(m)$. The superpotential $v_{m-1}(x, t, \lambda_m)$ relating such a pair of isospectral Schrödinger systems can always be obtained from the appropriate superpotential $v_m^{(as)}(x, t)$ corresponding to the associated irreducible extended Schrödinger system by one of the limits of the form $\lim_{C_m \to 0, \infty} v_m^{(as)}(x, t) = \pm v_{m-1}(x, t, \lambda_m)$ [12,28]. The spectrum of the corresponding Dirac Hamiltonian $\mathcal{D}_m$ (supercharge $\mathcal{S}_{m,1}$) with the scalar potential $v_{m-1}(x, t, \lambda_m)$ is symmetric with a central gap between bound states or continuous bands; it can only contain defects of the kink-antikink type, and never kink type defects. For such extended Schrödinger systems, the differential order of the integrals $\mathcal{P}_a$ and $\mathcal{Q}_a$ will reduce by two. From the point of view of the limit of the associated appropriate irreducible system $\mathcal{L}_m^{(as)}$, we have $\mathcal{L}_m^{(as)} \to \mathcal{L}_m$, and then one can find that $\mathcal{P}_m^{(as)} \to \mathcal{L}_m \mathcal{P}_m$, and a similar relation for the supercharges $\mathcal{Q}_a$. The indicated reducibility of the matrix differential operators $\mathcal{P}_a$ and $\mathcal{Q}_a$ does not affect the nature of the supersymmetry: the corresponding extended Schrödinger system presented by the 2×2 diagonal matrix Hamiltonian operator $\mathcal{L}_m$ is characterized by the exotic

nonlinear $N = 4$ supersymmetry generated by two first-order supercharges $\mathcal{S}_a$ and by two fermionic integrals $\mathcal{Q}_a$ that are higher (even)-order differential operators, and by two bosonic integrals composed of the Lax-Novikov integrals of the completely isospectral Schrödinger subsystems.

VI. SOLITON SOLUTIONS FOR THE mKdV EQUATION

In the next two subsections, we discuss briefly the mKdV solutions corresponding to the multi-kink-antikink solitons propagating over the asymptotically free kink or kink-antikink backgrounds, and then we consider a much more rich case corresponding to solutions in the crystalline kink and kink-antikink backgrounds.

A. Multi-kink-antikink solutions over a kink background

The employment of the multisoliton solutions of the KdV equation constructed on the basis of the initial trivial solution $u = 0$ allows us to find topologically nontrivial solutions $v^K(x, t)$ for the mKdV equation with the asymptotic behavior $v^K(+\infty, t) = -v^K(-\infty, t) = \text{const} \neq 0$. The index K reflects the kink type nature of the solutions. To obtain the mKdV solutions with the indicated asymptotic behavior, we should take u_m with one more bound state in the spectrum of the associated Shrödinger system in comparison with the $(m - 1)$ bound states supported by the potential u_{m-1}. In this case, the solution to the mKdV equation will have a form of the multi-kink-antikink defect propagating over the kink. The kink-antikink perturbations will always have amplitudes smaller than the kink amplitude, characterized by the parameter κ_m, due to the ordering $0 < \kappa_1 < \cdots < \kappa_m$. The kink-antikinks ($j = 1, \ldots, m - 1$) and kink ($j = m$) propagate to the left with the velocities $\mathcal{V}_j = 4\kappa_j^2 - 6\kappa_m^2$. So, the kink's speed is the lowest, being equal to $2\kappa_m^2$, while the kink-antikink solitons with lower amplitudes have higher speeds. Such solutions generalize the mKdV kink solution $v_0^K(x, t) = \kappa \tanh \kappa(x + 2\kappa^2 t)$, and analytically they are given by

$$v_{m-1}^K(x, t) = V_m^K(x + 6\kappa_m^2 t, t), \tag{6.1}$$

where, in correspondence with Eq. (2.22),

$$V_m^K(x, t) = \Omega_{m-1}^K(x, t) - \Omega_m^K(x, t),$$
$$\Omega_m^K = -(\log W(\cosh X_1^-, \sinh X_2^-, \ldots, f(X_m^-)))_x. \tag{6.2}$$

$f(X_m^-) = \sinh X_m^-$ if m is even, $f(X_m^-) = \cosh X_m^-$ if m is odd, and X_m^- is defined in Eq. (2.22). The functions $\pm v_m^K(x, t)$ (representing solutions for the defocusing mKdV equation) are of the kink type with m solitons that deform the moving kink (or antikink) background in their
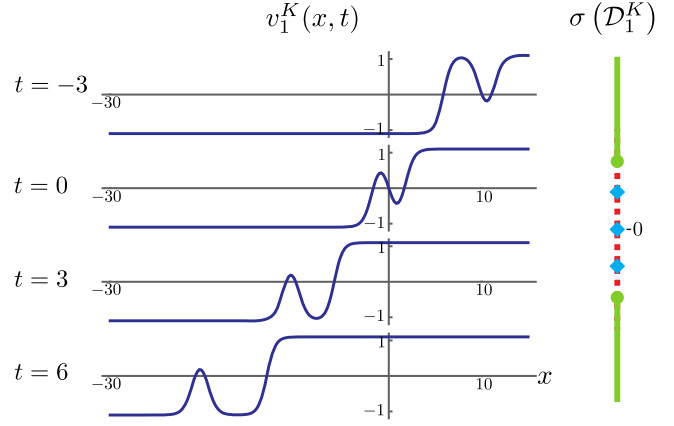

$$v_1^K(x, t) \qquad\qquad \sigma(\mathcal{D}_1^K)$$

FIG. 6 (color online). Solution of the mKdV equation representing the kink-antikink (characterized by the κ_1 parameter) propagation over the kink (given by κ_2) background, both moving to the left. When the soliton (which is faster) is to the right of the kink center (see the $t = -3$ instant), it has a form of the antikink-kink perturbation. Overtaking the kink center, it flips and transforms into the kink-antikink perturbation ($t = 3$ and $t = 6$). Here $\kappa_1 = 1$, $\kappa_2 = 1.1$, $x_{0i} = 0$, and $i = 1, 2$. The change $v \to -v$ provides a solution over the antikink background with a mutual transform of the antikink-kink and kink-antikink perturbations. The kink has a bigger amplitude $2\kappa_2$ equal to the distance between asymptotes, and this value also corresponds to the size of the central gap in the spectrum of the associated Dirac Hamiltonian operator shown on the right. Filled circles correspond to nondegenerate energy levels at the edges of the doubly degenerate continuous parts of the spectrum, while blue squares indicate nondegenerate bound states inside the spectral gap. The zero-energy bound state is associated with the kink; the two other bounds states are associated with the kink-antikink perturbation in the mKdV solution.

propagation without overpassing its asymptotes. An example of a such solution is represented in Fig. 6.

B. Multi-kink-antikink solutions over the topologically trivial background

The multi-kink-antikink solutions propagating over the topologically trivial background with the asymptotic behavior $v(-\infty, t) = v(+\infty, t) = \text{const} \neq 0$ can be obtained from the KdV solutions u_m and u_{m-1} which, as the Schrödinger potentials, support the same number [$(m-1)$, $m = 2, \ldots$] of bound states with coinciding energies. In such a pair, the potentials u_m and u_{m-1} are related by the Darboux transformation that displaces solitons [12,28]. They generalize the simplest kink-antikink solution for the mKdV equation,

$$v_0(x, t) = -\kappa_1, \tag{6.3}$$

which corresponds to the nonzero mass term $m = \kappa_1$ of the free Dirac Hamiltonian operator $\mathcal{D}_0$; see Eq. (5.6).

The simplest generalization of Eq. (6.3) is given by

$$v_1(x, t) = \kappa_1 \tanh\left(\kappa_1(x + \nu t)\right)$$
$$- \kappa_1 \tanh\left(\kappa_1(x + \nu t) - \Delta\right) - \kappa_1 \coth \Delta, \quad (6.4)$$

where $\nu = 6\kappa_2^2 - 4\kappa_1^2 > 0$, $\Delta = \frac{1}{2}\log\left(\frac{\kappa_2 + \kappa_1}{\kappa_2 - \kappa_1}\right) > 0$, and $\kappa_2 > \kappa_1 > 0$. The mKdV solution (6.4) is related to the mutually displaced one-soliton KdV solutions $u_1(x, t)$ and $u_2(x, t)$ via the Miura transformation, $u_1 = v_1^2 + v_1' = \kappa_2^2 - 2\kappa_1^2 \text{sech}^2(\kappa_1(x + \nu t))$, $u_2 = v_1^2 - v_1' = \kappa_2^2 - 2\kappa_1^2 \text{sech}^2(\kappa_1(x + \nu t) - \Delta)$. The analytic form of this type of the solutions is given by relations of the same form as Eqs. (6.1)–(6.2) but with $f(X_m^-)$ changed here for $f(X_m^-) = \exp X_m^-$. Such solutions can be obtained from the topologically nontrivial solutions (6.2) by taking there a limit $x_{0m} \to +\infty$ or $-\infty$, which corresponds to sending the soliton (kink) associated with the nondegenerate zero energy in the spectrum of $\mathcal{D}$ to $+\infty$ or $-\infty$. Thus, the velocities of the remaining kink-antikink solitons with $j = 1, \dots, m-1$ are the same ($\mathcal{V}_j = 4\kappa_j^2 - 6\kappa_m^2$) as in the solutions with the kink, indexed there by $j = m$, and its traces are still present here by restricting the amplitudes of the kink-antikinks and their speeds. An example of such a type of solutions is shown in Fig. 7.
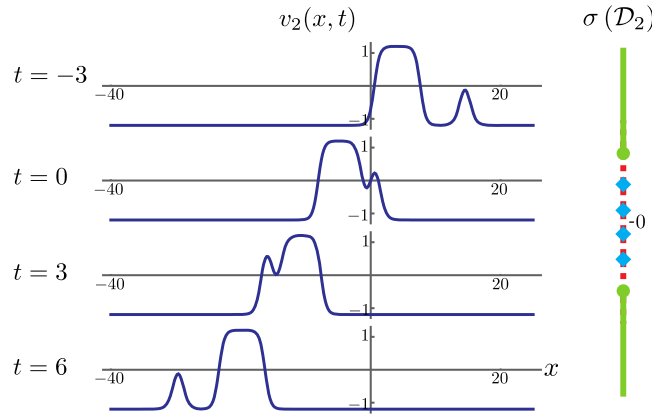

FIG. 7 (color online). Solution of the mKdV equation corresponding to two kink-antikink perturbations propagating to the left. Here $\kappa_1 = 1$, $\kappa_2 = 1.2$, $\kappa_3 = 1.2 + 10^{-7}$, $x_{0i} = 0$, and $i = 1$, 2, 3. $2\kappa_3$ corresponds to the size of the gap in the spectrum of the Dirac Hamiltonian operator, and κ_2 defines a bigger kink-antikink soliton; the closeness of its value to κ_3 causes this soliton to be higher and wider, and defines the energies $\pm\sqrt{\kappa_3^2 - \kappa_2^2}$ of the two bound states supported by this defect. κ_1 defines the parameters of the smaller kink-antikink soliton and the energies $\pm\sqrt{\kappa_3^2 - \kappa_1^2}$ of the two bound states supported by it. In contrast with the KdV solutions with a free background, the defects with smaller amplitudes propagate with higher speed. A nonzero asymptotic value of this type of solution corresponds to a constant mass term in a free massive Dirac Hamiltonian operator.

C. Kink-antikink pulse type defects in a crystalline kink background

On the basis of the stationary cnoidal solution for the KdV equation from Sec. III, one can construct diverse types of solutions for the mKdV equation, some of which are topologically trivial, while others have a nontrivial topological nature. If we use as u_{m-1} a solution $u_{m-1,0}$ of the KdV equation that contains only the potential-well soliton defects in the periodic background, and take $u_m = u_{m,0}$ of the same type but with one additional pulse soliton defect, then the associated solution v_m of the mKdV equation will describe multiple kink-antikink perturbations propagating in a moving crystal kink; see Fig. 8. The kink here is the defect of the greatest amplitude. Together with other soliton defects, it propagates to the left; see Sec. VI J below. In this case the solutions can be presented in the form

$$v_{0,m-1}^K(x, t) = V_{0,m}^K(x - 6\lambda(\beta_m^- + i\mathbf{K}')t, t), \quad (6.5)$$
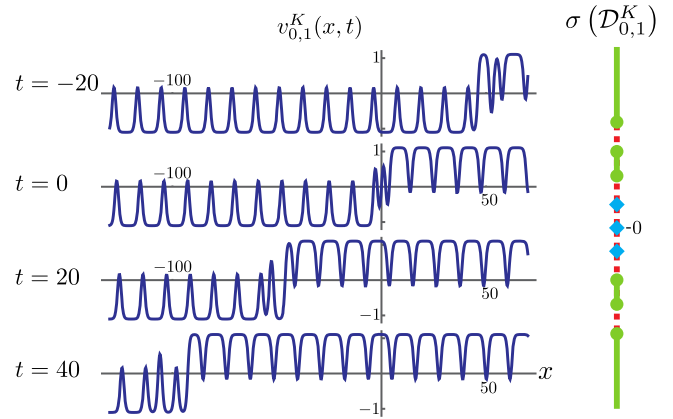

FIG. 8 (color online). Kink-antikink (given by β_1^-) and a kink (given by β_2^-) type defects propagating over a kink-antikink crystalline background. This mKdV solution with $\mu = 1$, $k = 0.999$, $\beta_1^- = 1.7$, $\beta_2^- = 1.5$, and $C_i^- = 1$, $i = 1$, 2 is somewhat analogous to that presented in Fig. 6. The kink perturbation and the kink-antikink in the form of a pulse (pul) soliton defect as well as the kink-antikink crystalline background (bg) move to the left, and the magnitudes of their velocities (speeds) are subject here to the relation $0 < |\mathcal{V}_{\text{kink}}| < |\mathcal{V}_{\text{pul}}| < |\mathcal{V}_{\text{bg}}|$; see Sec. VI J below. The pulse soliton defect flips when it passes from one side of the crystalline kink defect to another. Notice that in contrast to the present case, for the mKdV solution depicted in Fig. 6 the background is given there by constant asymptotes for which a state of motion is not defined. The size of a central gap in the spectrum of the associated Dirac Hamiltonian operator shown on the right is given by $2\mu|\text{dn}(\beta_2^- + i\mathbf{K}'|k)|$. The energies of the two bound states trapped by the kink-antikink defect are given by $E_\pm(\alpha) = \pm\mu\sqrt{\text{dn}^2(\alpha|k) - \text{dn}^2(\beta_2^- + i\mathbf{K}'|k)}$ with $\alpha = \beta_1^- + i\mathbf{K}'$, while the zero-energy value, $E_\pm(\alpha = \beta_2^- + i\mathbf{K}') = 0$, corresponds to a unique bound state trapped by the kink defect. The edges of the allowed bands correspond to $\alpha = 0$, $\mathbf{K}$, $\mathbf{K} + i\mathbf{K}'$.

where

$$V_{0,m}^K(x,t) = \Omega_{0,m-1}^K(x,t) - \Omega_{0,m}^K(x,t),$$
$$\Omega_{0,m}^K = -(\log W(\mathcal{F}_+(1), \mathcal{F}_-(2), \ldots, \mathcal{F}_{(-1)^{m+1}}(m)))_x,$$
(6.6)

and $\lambda(\alpha) = \mu^2(\mathrm{dn}^2(\alpha|k) - \frac{1}{3}(1+k'^2))$. The spectrum of $\mathcal{D}$ is symmetric, with two finite and two semi-infinite allowed bands. It contains a finite number of bound states in the central gap, and one of these bound states is exactly in the center ($E = 0$), while two other gaps are unoccupied.

D. Multi-kink-antikink pulse type defects in a kink-antikink crystal background

Let us take a solution $u_{m-1,0}$ of the KdV equation as a solution u_{m-1} in Eq. (5.3), and choose u_m in the form of the solution of the same type, $u_m = \tilde{u}_{m-1,0}$, but displaced by means of the Darboux transformation. Then we get the associated solution v_m of the mKdV equation in the form of multi-kink-antikink defects propagating in a crystalline background. In this case, again, both the crystalline background as well as the pulse defects will propagate to the left. Such a type of solutions can be presented in the analytical form
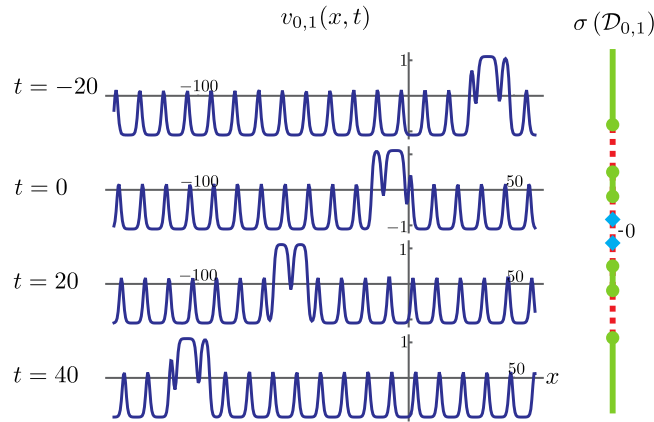

FIG. 9 (color online). A kink-antikink pulse (given by β_1^-) over a kink-antikink crystalline background. Here $\mu = 1$, $k = 0.9999$, $\beta_1^- = 1.5 + 10^{-12}$, $\beta_2^- = 1.5$, and $C_i^- = 1$, $i = 1, 2$. When the values of β_1^- and β_2^- are closer, the kink-antikink defect in the background of the kink-antikink crystal is more notable. Both the kink-antikink pulse and the kink-antikink crystal background move to the left, and the speed of the latter is higher than that of the defect. The size of a central gap in the spectrum of the associated Dirac Hamiltonian operator shown on the right is given by $2\mu|\mathrm{dn}(\beta_2^- + i\mathbf{K}'|k)|$. The energies of the bound states trapped by the defect are $E_\pm(\alpha) = \pm\mu\sqrt{\mathrm{dn}^2(\alpha|k) - \mathrm{dn}^2(\beta_2^- + i\mathbf{K}'|k)}$ with $\alpha = \beta_1^- + i\mathbf{K}'$, and they are represented by the blue rectangles. The nondegenerate energy values of the edges of the allowed bands correspond to $\alpha = 0$, $\mathbf{K}$, $\mathbf{K} + i\mathbf{K}'$.

$$v_{0,m-1} = V_{0,m}(x - 6\lambda(\beta_m^- + i\mathbf{K}')t, t), \quad (6.7)$$

where

$$V_{0,m}(x,t) = (\log W(\mathcal{F}_+(1), \mathcal{F}_-(2), \ldots, \mathcal{F}_{(-1)^m}(m-1)))_x$$
$$- (\log W(\mathcal{F}_+(1), \mathcal{F}_-(2), \ldots, \mathcal{F}_{(-1)^m}(m-1), F(x,t,\beta_m^-)))_x.$$
(6.8)

The function $F(x,t,\beta_m^-)$ is defined here by Eq. (4.1). The spectrum of $\mathcal{D}$ is symmetric, with two finite and two semi-infinite allowed bands. It has a finite even number of bound states in the central gap, and so (in contrast with the previous case) there is no bound state of discrete zero energy in the center of the gap. As in the class of solutions discussed in the previous section, the symmetric noncentral gaps do not contain bound states. The mKdV solutions of this type can be obtained from those described in the preceding section by sending the kink to plus or minus infinity; the concrete analytic form (6.8) corresponds to taking the limit $C_m^- \to \infty$ in the solution (6.5). This case is illustrated in Fig. 9.

E. Multi-kink-antikink compression modulation defects over a kink in a kink-antikink crystal background

There are no nonsingular solutions of the mKdV equation associated with the KdV solutions which in the Darboux-Crum construction use only the states from the gap. To get nonsingular solutions, one can employ in the construction of u_m a state from the forbidden lower band of the Lamé system in addition to the states from the gap employed for the construction of u_{m-1}, or to generate a nonlinear displacement by means of the Darboux transformation. In the first case we obtain a solution for the mKdV equation which contains a kink in a background, while in the second case there will be no such kink in the structure of the mKdV solution. The solution of the first indicated case takes the form

$$v_{2l,0}^K = V_{2l,1}^K(x - 6\lambda(\beta_1^- + i\mathbf{K}')t, t), \quad (6.9)$$

where

$$V_{2l,1}^K(x,t)$$
$$= (\log W(\Phi_+(1), \Phi_-(2), \ldots, \Phi_+(2l-1), \Phi_-(2l), \mathcal{F}_+(1)))_x$$
$$- (\log W(\Phi_+(1), \Phi_-(2), \ldots, \Phi_+(2l-1), \Phi_-(2l)))_x.$$
(6.10)

In this solution, the defects of the compression modulation type propagate over a kink defect, which, in turn, propagates over the crystalline background by deforming it. An example of such a solution is shown in Fig. 10. Here, the kink, the background, and the compression modulation type defects move to the left. The shown solution possesses
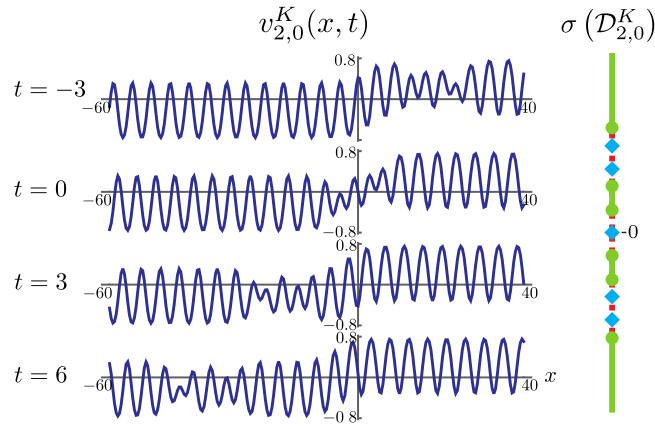
$$v_{2,0}^K(x,t) \qquad \sigma\left(\mathcal{D}_{2,0}^K\right)$$

FIG. 10 (color online). The mKdV solution with two kink-antikink modulations (given by β_1^+ and β_2^+) and a kink (given by β_1^- and corresponding to the KdV pulse soliton) propagating in a kink-antikink crystal background. Here $\mu = 1$, $k = 0.9$, $\beta_1^- = 1.8$, $\beta_1^+ = 1$, $\beta_2^+ = 1.3$, and $C_1^- = C_1^+ = C_2^+ = 1$, and the velocity magnitudes of the solitons of the compression modulations (mod) type, of the background (bg), and the kink soliton are subject to the inequalities $|\mathcal{V}_{\text{mod}}| > |\mathcal{V}_{\text{bg}}| > |\mathcal{V}_{\text{kink}}| > 0$; see Sec. VI J below. The size of the central gap in the spectrum of the associated Dirac Hamiltonian operator, shown on the right, is equal to $2\mu|\text{dn}(\beta_1^- + i\mathbf{K}'|k)|$. The energies of the bound states trapped by the kink-antikink modulations are given by $E_\pm(\alpha) = \pm\mu\sqrt{\text{dn}^2(\alpha|k) - \text{dn}^2(\beta_1^- + i\mathbf{K}'|k)}$ with $\alpha = \beta_1^+, \beta_2^+$, while the bound state of zero energy ($\alpha = \beta_1^- + i\mathbf{K}'$) is trapped by the kink defect. The edges of the allowed bands in the spectrum correspond to $\alpha = 0$, $\mathbf{K}$, $\mathbf{K} + i\mathbf{K}'$.

an even number of compression modulation defects. The solutions with an odd number of modulation defects can be obtained by applying the procedures explained earlier for the KdV equation. The spectrum of $\mathcal{D}_{2l,0}^K$ is symmetric, with two finite allowed bands and two semi-infinite allowed bands. Besides, it has a finite number of bound states in the external gaps, and one bound state of zero energy in the central gap.

F. Multi-kink-antikink compression modulation solutions in a kink-antikink crystal background

If the difference between u_m and u_{m-1} is a nonlinear displacement generated by a Darboux transformation, and if these solutions of the KdV equation are the compression modulation type defects, then the associated solution of the mKdV equation will be a kink-antikink crystal background propagating to the left, in which we have kink-antikink defects of the modulation type also moving to the left. Analytically, such solutions are given by

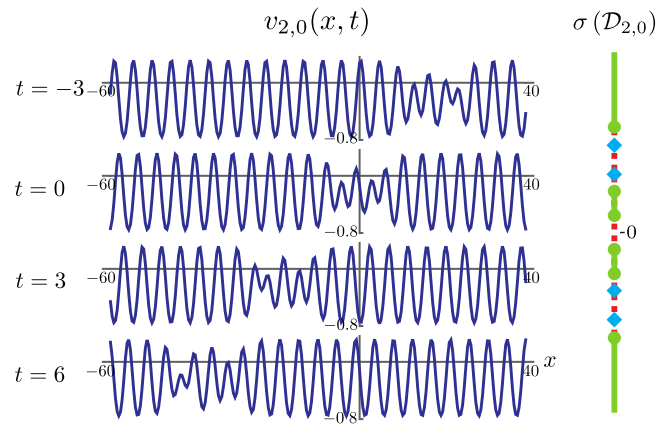$$v_{2l,0} = V_{2l,1}(x - 6\lambda(\beta_1^- + i\mathbf{K}')t, t), \qquad (6.11)$$

where

$$v_{2,0}(x,t) \qquad \sigma\left(\mathcal{D}_{2,0}\right)$$

FIG. 11 (color online). The mKdV solution with two kink-antikink modulations (given by β_1^+ and β_2^+) propagating over a kink-antikink crystal background (described by the parameter β_1^-). Here $\mu = 1$, $k = 0.9$, $\beta_1^- = 1.8$, $\beta_1^+ = 1$, $\beta_2^+ = 1.3$, and $C_{1,2}^+ = 1$. At $t = 0$, the vertical axis ($x = 0$) is shifted a little bit to the left with respect to the symmetry axis of the figure. This is due to the limit $C_1^- \to \infty$ applied to the solution shown in Fig. 10, the present solution. This limit corresponds to sending the kink to infinity and generates the displacements (phase shifts) in the background and in the remaining defects. The size of the central gap in the spectrum of the associated Dirac Hamiltonian operator is equal to $2\mu|\text{dn}(\beta_1^- + i\mathbf{K}'|k)|$. The energies of the bound states trapped by the kink-antikink modulation defects are given by $E_\pm(\alpha) = \pm\mu\sqrt{\text{dn}^2(\alpha|k) - \text{dn}^2(\beta_1^- + i\mathbf{K}'|k)}$ with $\alpha = \beta_1^+$, β_2^+. The edges of the allowed bands correspond to $\alpha = 0$, $\mathbf{K}$, $\mathbf{K} + i\mathbf{K}'$. The compression defects are more rapid than the background.

$$V_{2l,1}(x,t)$$
$$= (\log W(\Phi_+(1), \Phi_-(2), \ldots, \Phi_+(2l-1), \Phi_-(2l), F(x,t,\beta_1^-)))_x$$
$$- (\log W(\Phi_+(1), \Phi_-(2), \ldots, \Phi_+(2l-1), \Phi_-(2l)))_x.$$
$$(6.12)$$

Notice a difference in the last argument of the Wronskian in the first term on the right in Eq. (6.12) in comparison with Eq. (6.10). It reflects the fact that the solutions of the present type can be obtained from those discussed in the preceding section by sending the kink to infinity, by taking the limit $C_1^- \to \infty$ in Eq. (6.10).

Figure 11 shows the case with an even number of compression modulations defects. The case with an odd number of such defects can be obtained by the procedures explained earlier for the KdV system. The spectrum of $\mathcal{D}_{2l,0}$ is symmetric, with a finite number of bound states appearing in noncentral gaps, and with no bound states in the central gap.

G. Multi kink-antikink modulation solitons in a kink crystal

There is a special case which can be obtained as a limit from the solutions discussed in the preceding section. It is
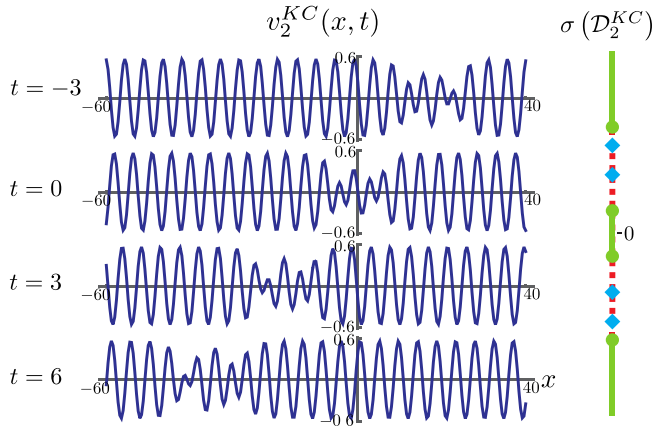
FIG. 12 (color online). The mKdV solution with two kink-antikink modulations (given by β_1^+ and β_2^+) over a kink crystal. Here, $\mu = 1$, $k = 0.9$, $\beta_1^+ = 1$, $\beta_2^+ = 1.3$, $\beta_1^- = \mathbf{K}$, and $C_1^- = C_{1,2}^+ = 1$. In this case there is no central gap in the spectrum of the associated Dirac Hamiltonian operator. The energies of the bound states trapped by the modulation defects are given by $E_\pm(\alpha) = \pm\mu\,\mathrm{dn}(\alpha|k)$ with $\alpha = \beta_1^+, \beta_2^+$, while the values $\alpha = 0$, $\mathbf{K}$ correspond to the edges of the allowed bands. In the kink crystal background, only the modulation type kink-antikink defects can exist, and they propagate to the left more rapidly than the kink crystal background. In this configuration, the velocity magnitude of the background, $|\mathcal{V}_{\mathrm{bg}}| = 2\mu^2(1 + k'^2)$, is minimal in comparison with those in other types of mKdV solutions.

generated by the choice of the solution u_{m-1} of the KdV equation which contains only compression modulation defects, while the additional state $\Psi \propto \mathrm{dn}(\mu x|k)$ employed for the construction of u_m is at the edge of the lower forbidden band of the associated one-gap Lamé system.[2] In this case the crystalline background in the mKdV solution is centered (vertically) at zero in contrast with the previously considered cases where it was displaced up or down. This centered crystalline background is known as the kink crystal solution which appears in the Gross-Neveu model [16,17]. In comparison with the previous cases, here in the spectrum of $\mathcal{D}$ the central gap (together with the bound states there) disappears and two finite continuous bands merge into one central allowed band centered at zero. So in this case one can have defects only of the compression modulation type; see Fig. 12. Here, as in the previous cases, the indicated soliton defects move to the left like the kink crystal propagating with the velocity $6\lambda(\mathbf{K} + i\mathbf{K}')$; see Sec. VI J below. The analytic form of this type of mKdV solutions is given by

$$v_{2l}^{\mathrm{KC}} = V_{2l}^{\mathrm{KC}}(x - 6\lambda(\mathbf{K} + i\mathbf{K}')t, t), \qquad (6.13)$$

---

[2]This is the ground state of the Lamé system at the lower edge of its valence band.

where

$$
\begin{aligned}
V_{2l}^{\mathrm{KC}}(x,t) = (&\log W(\Phi_+(1), \Phi_-(2), ..., \Phi_+(2l-1), \\
&\Phi_-(2l), \mathrm{dn}(\mu x|k)))_x \\
&- (\log W(\Phi_+(1), \Phi_-(2), ..., \Phi_+(2l-1), \\
&\Phi_-(2l)))_x.
\end{aligned} \qquad (6.14)
$$

In the simplest case $l = 0$ the solution is just the kink crystal

$$v_0^{\mathrm{KC}}(x,t) = (\log \mathrm{dn}(\mu(x - \mathcal{V}_{\mathrm{bg}}t)|k))_x \qquad (6.15)$$

propagating to the left with velocity $\mathcal{V}_{\mathrm{bg}} = -2\mu^2(1 + k'^2) < 0$.

H. Mixed multi-kink-antikink solitons over a kink in a kink-antikink crystal background

In a more general case, one can have both types of defects—compression modulations as well as pulse solitons—propagating over a moving crystal background. Depending on whether the difference between the u_{m-1} and u_m solutions of the KdV equation is a pulse type soliton or a nonlinear displacement, a kink defect will or will not appear in the kink-antikink crystal background. In the case when the indicated difference is a pulse type defect, the solutions over the kink crystalline background take the form

$$v_{2l,m-1}^K = V_{2l,m}^K(x - 6\lambda(\beta_m^- + i\mathbf{K}')t, t), \qquad (6.16)$$

where

$$
\begin{aligned}
V_{2l,m}^K(x,t) = (&\log W(\Phi_+(1), \Phi_-(2), ..., \Phi_-(2l), \\
&\mathcal{F}_+(1), \mathcal{F}_-(2), ..., \mathcal{F}_{(-1)^{m+1}}(m)))_x \\
&- (\log W(\Phi_+(1), \Phi_-(2), ..., \Phi_-(2l), \\
&\mathcal{F}_+(1), \mathcal{F}_-(2), ..., \mathcal{F}_{(-1)^m}(m-1)))_x \quad (6.17)
\end{aligned}
$$

is a modulated kink. In this solution, the kink, the pulse, and modulation type defects as well as the crystalline background move to the left.

The solution shown in Fig. 13 possesses an even number of compression modulation defects. Again, solutions with an odd number of defects of this type can be obtained by means of any of the procedures discussed in Sec. IV B. The spectrum of the Dirac Hamiltonian operator $\mathcal{D}$ in this case is symmetric. Besides the continuous bands shown in the figure, it contains a finite number of bound states in the external and central gaps. Besides, there is an additional bound state of zero energy in the center of the central gap, which is associated with the crystalline kink.
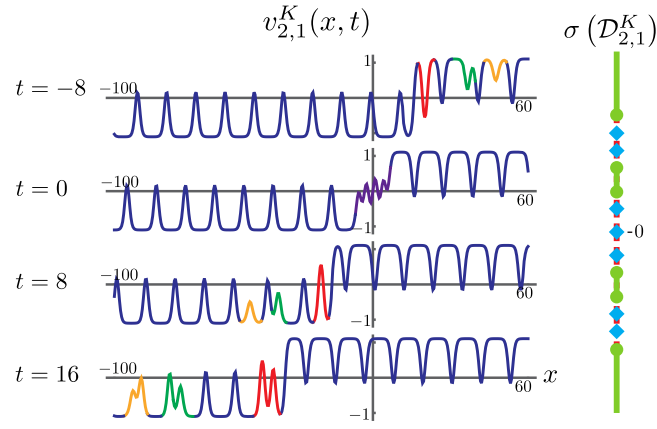
FIG. 13 (color online). The mKdV solution with a kink-antikink pulse (given by β_1^- and highlighted in red) and two kink-antikink modulations (given by β_1^+ and β_2^+ and shown in orange and green, respectively) propagating over a kink defect (β_2^-), with all of these defects propagating in a moving kink-antikink crystal background. Here $\mu = 1$, $k = 0.999$, $\beta_1^- = 1.7$, $\beta_2^- = 1.5$, $\beta_1^+ = 1$, $\beta_2^+ = 1.3$, and $C_{1,2}^\pm = 1$, and the magnitudes of the velocities of the defects and background are subject to the inequalities $|\mathcal{V}_{\mathrm{mod}}| > |\mathcal{V}_{\mathrm{bg}}| > |\mathcal{V}_{\mathrm{pul}}| > |\mathcal{V}_{\mathrm{kink}}| > 0$. The size of the central gap in the spectrum of the associated Dirac Hamiltonian operator is $2\mu|\mathrm{dn}(\beta_2^- + i\mathbf{K}'|k)|$. The energies of the bound states trapped by the modulation defects are given by $E_\pm(\alpha) = \pm\mu\sqrt{\mathrm{dn}^2(\alpha|k) - \mathrm{dn}^2(\beta_2^- + i\mathbf{K}'|k)}$ with $\alpha = \beta_1^+, \beta_2^+$. The energies in the central gap, which are marked by two blue squares symmetric with respect to the zero level, are given by $\alpha = \beta_1^- + i\mathbf{K}'$ and correspond to the bound states trapped by the kink-antikink pulse; the zero-energy value, $E_\pm(\alpha = \beta_2^- + i\mathbf{K}') = 0$, corresponds to a unique bound state trapped by the kink defect. The edges of the allowed bands correspond to $\alpha = 0$, $\mathbf{K}$, $\mathbf{K} + i\mathbf{K}'$.

I. Mixed multi-kink-antikink defects in a kink-antikink crystal background

If, unlike the previous case, the difference between u_{m-1} and u_m is given by a nonlinear displacement, there is no kink structure in the corresponding mKdV solution given by

$$v_{2l,m-1} = V_{2l,m}(x - 6\lambda(\beta_m^- + i\mathbf{K}')t, t), \tag{6.18}$$

where

$$V_{2l,m}(x,t) = (\log W(\Phi_+(1), \Phi_-(2), ..., \Phi_-(2l),$$
$$\mathcal{F}_+(1), \mathcal{F}_-(2), ..., \mathcal{F}_{(-1)^m}(m-1), F(x,t,\beta_m^-)))_x$$
$$- (\log W(\Phi_+(1), \Phi_-(2), ..., \Phi_-(2l),$$
$$\mathcal{F}_+(1), \mathcal{F}_-(2), ..., \mathcal{F}_{(-1)^m}(m-1)))_x \tag{6.19}$$

is a kink-antikink crystal background displaced from zero in the vertical direction and perturbed by propagating mixed multi-kink-antikink defects within it. An example
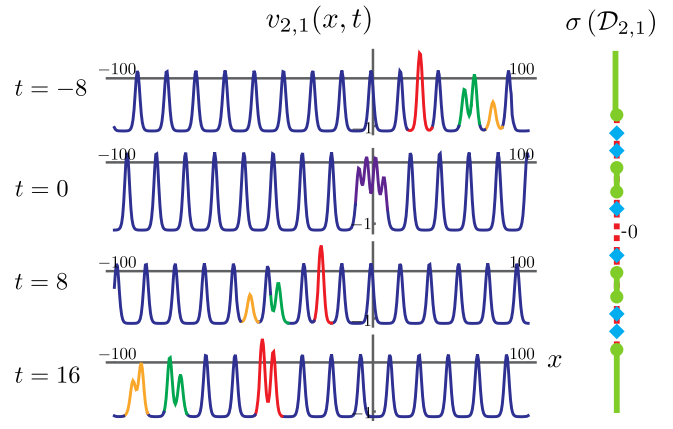

FIG. 14 (color online). The mKdV solution with a kink-antikink pulse (given by β_1^- and shown in red) and two kink-antikink modulations (given by β_1^+ and β_2^+ and highlighted in orange and green, respectively) propagating to the left in a kink-antikink crystal background that is moving to the left. Here $\mu = 1$, $k = 0.999$, $\beta_1^- = 1.5 + 10^{-10}$, $\beta_2^- = 1.5$, $\beta_1^+ = 1$, $\beta_2^+ = 1.3$, and $C_{1,2}^\pm = 1$, and the velocity magnitudes are subject to the inequalities $|\mathcal{V}_{\mathrm{mod}}| > |\mathcal{V}_{\mathrm{bg}}| > |\mathcal{V}_{\mathrm{pul}}| > 0$. The energies in the spectrum of the associated Dirac Hamiltonian operator are given by expressions similar to those in Fig. 9.

of such a solution is depicted in Fig. 14. The symmetric spectrum of $\mathcal{D}$ has a finite number of bound states in the central and external gaps, with no state of zero energy in the center of the central gap. The mKdV solutions of this type can be obtained from those discussed in the preceding section by sending the kink defect to infinity.

J. Velocities in the mKdV solutions with crystalline backgrounds

The mKdV solutions v_{m-1} are obtained on the basis of the Darboux construction of KdV solutions. The necessary step of the procedure, as we have seen, involves the Galilean transformation, $x \rightarrow x - 6\lambda_m t$. The boost parameter $G = 6\lambda_m$ of this transformation is given by the energy λ_m that corresponds to the nonphysical eigenstate of the one-gap Lamé system $L_{0,0}$ which is used to obtain the potential u_m with one more bound state in comparison with the partner potential u_{m-1}. Or, this λ_m corresponds to the eigenstate with the help of which the potential u_m is obtained from the completely isospectral potential u_{m-1} by means of the nonlinear Darboux displacement. In both cases $\lambda_m = \lambda(\beta_m^- + i\mathbf{K}')$, and β_m^- in the first case is associated with the mKdV kink supporting a bound state of a nondegenerate discrete zero-energy eigenvalue in the spectrum of the Dirac Hamiltonian operator $\mathcal{D}$, or, if there is no discrete zero-energy value in the spectrum of $\mathcal{D}$, β_m^- can be associated with the kink defect sent to infinity. This β_m^- corresponds to the eigenstate of minimal energy from the lower semi-infinite forbidden band in the spectrum of $L_{0,0}$ which is used in the Darboux-Crum transformations to

construct u_m, or to the eigenvalue of the "virtual" state from that band associated with the "kink sent to infinity." As a result, the crystalline background in the obtained mKdV solution propagates to the left and its velocity is

$$\mathcal{V}_{\text{bg}} = 6\lambda(\beta_m^- + i\mathbf{K}') = -2\mu^2(3\text{cs}^2(\beta_m^-|k^2) + 1 + k'^2) < 0. \tag{6.20}$$

The background propagates with a minimal speed in the class of the mKdV solutions with the kink crystal background, which were discussed in Sec. VI G. In that case $\beta_1^- = \mathbf{K}$ corresponds to the edge state $\text{dn}(\mu x|k)$ of $L_{0,0}$, and, therefore, $\mathcal{V}_{\text{bg}} = -2\mu^2(1 + k'^2) < 0$.

If the mKdV solution has pulse type defects that are different from the kink, their velocities are given by

$$\mathcal{V}_{\text{pul}}(\beta_j^-) = \mathcal{V}(\beta_j^-) + 6\lambda(\beta_m^- + i\mathbf{K}') < 0,$$
$$\mathbf{K} > \beta_j^- \geq \beta_m^-, \qquad j = 1, \ldots, m-1, \tag{6.21}$$

with $\mathcal{V}(\beta_j^-)$ given by Eq. (4.13). Analogously, the velocities of the modulation type defects, if they are present in the mKdV solution, are

$$\mathcal{V}_{\text{mod}}(\beta_j^+) = \mathcal{V}(\beta_j^+) + 6\lambda(\beta_m^- + i\mathbf{K}') < 0,$$
$$0 < \beta_j^+ < \mathbf{K}, \tag{6.22}$$

where $\mathcal{V}(\beta_j^+)$ are given by Eq. (4.14). In the case where the mKdV solution has a kink defect, its velocity is defined by a relation of the form (6.21) but with $j = m$, i.e.,

$$\mathcal{V}_{\text{kink}} = \mathcal{V}(\beta_m^-) + 6\lambda(\beta_m^- + i\mathbf{K}') < 0. \tag{6.23}$$

One can see that in the mKdV solution, the speeds of the background and defects (some of which can be absent in the solution) are ordered according to the inequalities $|\mathcal{V}_{\text{mod}}| > |\mathcal{V}_{\text{bg}}| > |\mathcal{V}_{\text{pul}}| > |\mathcal{V}_{\text{kink}}| > 0$.

VII. DISCUSSION AND OUTLOOK

We have constructed solutions to the KdV equation with an arbitrary number of solitons in a stationary asymptotically periodic background. In this case there exist two types of solitons:
  (i) potential-well defects (pulses), which propagate to the right;
  (ii) compression modulation defects, which move to the left.
These solutions asymptotically have the form of the one-gap Lamé potential but subjected to the phase shifts $x \to x - x_0^{\mp}$, $x_0^{\mp} = \pm\frac{1}{\mu}(\sum_i \beta_i^- + \sum_j \beta_j^+)$ for $x \to \mp\infty$ with respect to the stationary solution (3.1). The asymmetry in the propagation of the two types of soliton defects is valid in the case of a stationary background. If we apply Galilean transformations to the KdV solutions, we obtain new

solutions for which, in the general case, the described propagation asymmetry of the defects over the now moving background will be changed. However, this does not change the picture of the relative motion: pulse defects will always propagate to the right with respect to the asymptotically periodic background, while modulation type defects will move to the left with respect to a nonstationary crystalline background. An interesting peculiarity that we have also observed in the constructed KdV solutions is that in the limit cases when the amplitudes of the pulse and compression modulation defects tend to zero, the limit values of the velocities of defects with respect to the crystalline background are nonzero.

For the mKdV equation, we have constructed the following solutions from the obtained KdV solutions by means of the Miura-Darboux-Crum transformations:
  (i) solutions with a kink crystal background, in which there can exist only solitons in the form of the compression modulation type defects;
  (ii) solutions with a kink-antikink crystal background, in which there can exist kink-antikinks in the form of the pulse and/or compression modulations type defects.
In a kink-antikink crystal background there also can appear a topological defect in the form of a kink [or antikink, if we use a symmetry of the mKdV equation by changing $v(x, t)$ for $-v(x, t)$] which is always related to the KdV pulse type defect that traps the bound state with the lowest energy in the lower forbidden band in the spectrum of the associated perturbed one-gap Lamé system.

Unlike the KdV, the mKdV equation has no Galilean symmetry, and the velocities of the defects and asymptotically periodic background in the solutions we constructed have an absolute character.

In the mKdV solutions, all of the defects and crystalline backgrounds move to the left, and the velocity magnitudes of the kink-antikink defects of the modulation (mod) and the pulse (pul) types, and the velocity magnitudes of the background (bg) and the kink are subject to the inequalities $|\mathcal{V}_{\text{mod}}| > |\mathcal{V}_{\text{bg}}| > |\mathcal{V}_{\text{pul}}| > |\mathcal{V}_{\text{kink}}| > 0$. Thus, with taking into account the sign of the velocities, we have for the defects and backgrounds in the mKdV solutions (similarly to those in the KdV solutions) $(\mathcal{V}_{\text{pul}} - \mathcal{V}_{\text{bg}}) > 0$ and $(\mathcal{V}_{\text{mod}} - \mathcal{V}_{\text{bg}}) < 0$. At the same time, the velocity magnitude (speed) of the kink defect, if it is present in the mKdV solution, always has a minimal value in comparison with other velocity magnitudes.

The presence or absence of the kink in the mKdV solution is detected by the $N = 2$ supersymmetry of the associated extended Schrödinger system. It is generated by the first-order supercharge operators $\mathcal{S}_a$, $a = 1, 2$, which are similar in nature to the Dirac Hamiltonian operators with a scalar potential. When a kink is present or absent the supercharges do or do not have a zero mode, and the $N = 2$ supersymmetry is unbroken or broken. The supersymmetry also detects the case of the mKdV solutions with the kink

crystal background. For such solutions, the kernel of supercharges is two-dimensional. Unlike the solutions with a kink, the corresponding zero modes in this case are given not by normalizable but rather periodic states.[3] The position of the bound states in the gaps in the spectra of the supercharges also defines the type of defects present in the corresponding mKdV solution.

We have showed that the $N = 2$ supersymmetry constitutes a part of a more broad, $N = 4$ type exotic nonlinear supersymmetry, which includes in its structure two bosonic generators composed from the nontrivial Lax-Novikov integrals of the pair of Schrödinger subsystems. These bosonic generators are higher-derivative differential operators, one of which is the central element of the superalgebra. Besides, the exotic supersymmetric structure contains an additional pair of supercharges that are matrix differential operators of even order. The additional integrals appropriately reflect the peculiar nature of the extended Schrödinger system associated with the pair of KdV solutions by detecting all the bound states and the band-edge states in the spectrum, as well as distinguish the eigenstates corresponding to the fourfold degenerate energy values inside the allowed bands.

Both the KdV and mKdV equations are invariant under simultaneous inversion of the t and x variables, but not under a reflection of t (or, of x) only. The stationary trivial solution $u = 0$, on the basis of which we constructed soliton solutions over the asymptotically free background, is invariant under separate inversions in t and x. The same is true for the stationary cnoidal solution in the form of the stationary one-gap Lamé potential. So, the "initial data" in the construction are invariant under t inversions, and the anisotropy of evolution as well as the chiral asymmetry of the nonstationary solutions is rooted in the anisotropy of the equations themselves. Namely, in our construction—though the "seed" KdV solutions are time-inversion invariant—the solutions of the auxiliary problem in the Lax formulation for the KdV equation, which are generating elements for the Darboux-Crum transformations, break this symmetry. In the case of the asymptotically free background, in the indicated solutions of the auxiliary problem the dependence on time enters universally in the form of the arguments $x - \mathcal{V}_j t$ with $\mathcal{V}_j = 4\kappa_j^2 > 0$. As a result, all of the solitons in nonsingular KdV solutions move to the right. For the soliton solutions over an asymptotically periodic background, the third-order Lax operator of the initial Lamé system has eigenvalues of different signs on the upper and lower horizontal borders of the fundamental α rectangle which correspond to the lower forbidden band and the gap. It is this sign asymmetry that is ultimately responsible for chiral asymmetry in the

propagation of the KdV solutions in the form of pulse and compression modulation defects over a crystalline background. The asymmetry of the mKdV solutions is inherited from that for the KdV solutions.

Since the KdV and mKdV solutions (and particularly those associated with the Lamé quantum system) find many diverse applications in a variety of different areas of physics—ranging from hydrodynamics, plasma physics, and optics to hadron physics and cosmology [1,5,17,18,24,30,34–40]—it would be very interesting to find where the obtained new solutions could appear. They could appear in the form of perturbations of a different nature, which would propagate in a nonlinear media with different velocities and reveal chiral asymmetry in their dynamics. Another peculiarity which could be associated with the described solutions is the existence of nonzero bounds for the velocity of the defects with disappearing amplitudes.

It would also be interesting to consider a generalization of the approach employed here by using Darboux transformations for the first-order Hamiltonian operator of a $(1 + 1)$-dimensional Dirac system instead of the second-order Schrödinger operator. In this way one could get finite-gap Dirac Hamiltonian operators of the form

$$\mathcal{D} = \begin{pmatrix} V_2(x) & -\frac{d}{dx} + V_1(x) \\ \frac{d}{dx} + V_1(x) & -V_2(x) \end{pmatrix} \qquad (7.1)$$

with an asymmetric spectrum. The corresponding stationary potentials $V_{1,2}(x)$ could then be promoted to solutions in the form of the twisted kinks and twisted kink-antikinks [18,34,41,42] in a periodic background for a nonlinear Schrödinger equation belonging to the Zakharov-Shabat–Ablowitz-Kaup-Newell-Segur hierarchy.

In the supersymmetric quantum-mechanical structure we discussed, the $N = 4$ refers to the number of supercharges appearing in the extended Schrödinger system. As the extended system is composed of a pair of the perturbed one-gap Lamé systems, one could expect the appearance of only two supercharges as it happens in supersymmetric quantum-mechanical systems of a general nature [43]. The peculiarity of the considered systems consists in their finite-gap nature, and it is this property that is behind the extension of the usual $N = 2$ supersymmetry up to the exotic $N = 4$ nonlinear supersymmetric structure that incorporates the pair of Lax-Novikov integrals of the subsystems in the form of the two additional bosonic generators. It would be interesting to investigate whether the described exotic supersymmetric structure can be somehow related to the supersymmetric extensions of the KdV and mKdV equations and corresponding hierarchies that are considered within the superspace (superfield) generalizations of the indicated classical $(1 + 1)$-dimensional integrable systems [44–49].

---

[3]These zero modes are constructed from Darboux-dressed edge states $\mathrm{dn}(\mu x | k)$ and $\mathrm{dn}(\mu x + \mathbf{K} | k)$ of the pair of mutually shifted in the half-period Lamé systems by applying to them the Galilean boost with velocity $\mathcal{V}_{\mathrm{bg}} = -2\mu^2(1 + k'^2)$.

ACKNOWLEDGMENTS

[1] G. L. Lamb, *Elements of Soliton Theory* (Wiley, New York, 1980).

[2] S. P. Novikov, S. V. Manakov, L. P. Pitaevskii, and V. E. Zakharov, *Theory of Solitons* (Plenum, New York, 1984).

[3] A. J. Heeger, S. Kivelson, J. R. Schrieffer, and W.-P. Su, Rev. Mod. Phys. **60**, 781 (1988).

[4] P. Drazin and R. Johnson, *Solitons: An Introduction* (Cambridge University Press, Cambridge, England, 1996).

[5] Y. S. Kivshar and B. Luther-Davies, Phys. Rep. **298**, 81 (1998).

[6] *Classical and Quantum Nonlinear Integrable Systems. Theory and Applications*, edited by A. Kundu (Institute of Physics, London, 2003).

[7] Y. V. Kartashov, B. A. Malomed, and L. Torner, Rev. Mod. Phys. **83**, 247 (2011); **83**, 405(E) (2011).

[8] E. A. Kuznetsov and F. Dias, Phys. Rep. **507**, 43 (2011).

[9] I. Kay and H. E. Moses, J. Appl. Phys. **27**, 1503 (1956).

[10] V. B. Matveev and M. A. Salle, *Darboux Transformations and Solitons* (Springer-Verlag, Berlin, 1991).

[11] E. D. Belokolos, A. I. Bobenko, V. Z. Enol'skii, A. R. Its, and V. B. Matveev, *Algebro-Geometric Approach to Nonlinear Integrable Equations* (Springer-Verlag, Berlin, 1994).

[12] A. Arancibia, F. Correa, V. Jakubsky, J. M. Guilarte, and M. S. Plyushchay, Phys. Rev. D **90**, 125041 (2014).

[13] H. W. Braden and A. J. Macfarlane, J. Phys. A **18**, 3151 (1985).

[14] G. V. Dunne and J. Feinberg, Phys. Rev. D **57**, 1271 (1998).

[15] F. Correa, V. Jakubsky, L. M. Nieto, and M. S. Plyushchay, Phys. Rev. Lett. **101**, 030403 (2008).

[16] M. S. Plyushchay, A. Arancibia, and L. M. Nieto, Phys. Rev. D **83**, 065025 (2011).

[17] M. Thies and K. Urlichs, Phys. Rev. D **67**, 125015 (2003); M. Thies, Phys. Rev. D **69**, 067703 (2004).

[18] G. Basar and G. V. Dunne, Phys. Rev. Lett. **100**, 200404 (2008); Phys. Rev. D **78**, 065022 (2008).

[19] R. Anglani, R. Casalbuoni, M. Ciminale, N. Ippolito, R. Gatto, M. Mannarelli, and M. Ruggieri, Rev. Mod. Phys. **86**, 509 (2014).

[20] A. I. Larkin and Y. N. Ovchinnikov, Zh. Eksp. Teor. Fiz. **47**, 1136 (1964) [Sov. Phys. JETP **20**, 762 (1965)].

[21] P. Fulde and R. A. Ferrell, Phys. Rev. **135**, A550 (1964).

[22] A. Saxena and A. R. Bishop, Phys. Rev. A **44**, R2251 (1991).

[23] S. A. Brazovkii, S. A. Gordynin, and K. N. Kirova, Pis'ma Zh. Eksp. Teor. Fiz. **31**, 486 (1980) [JETP Lett. **31**, 456 (1980)].

[24] M. Thies and K. Urlichs, Phys. Rev. D **72**, 105008 (2005); O. Schnetz, M. Thies, and K. Urlichs, Ann. Phys. (Amsterdam) **321**, 2604 (2006).

[25] A. Arancibia, J. M. Guilarte, and M. S. Plyushchay, Phys. Rev. D **88**, 085034 (2013).

[26] E. T. Whittaker and G. N. Watson, *A Course of Modern Analysis* (Cambridge University Press, Cambridge, England, 1980).

[27] J. L. Burchnall and T. W. Chaundy, Proc. London Math. Soc., **s2-21**, 420 (1923); Proc. R. Soc. A **118**, 557 (1928).

[28] A. Arancibia and M. S. Plyushchay, Phys. Rev. D **90**, 025008 (2014).

[29] A. Hasegawa and F. Tappert, Appl. Phys. Lett. **23**, 171 (1973).

[30] A. Chabchoub, O. Kimmoun, H. Branger, C. Kharif, N. Hoffmann, M. Onorato, and N. Akhmediev, Phys. Rev. E **89**, 011002(R) (2014).

[31] R. M. Miura, J. Math. Phys. (N.Y.) **9**, 1202 (1968).

[32] F. Correa, V. Jakubsky, and M. S. Plyushchay, J. Phys. A **41**, 485303 (2008).

[33] A. Arancibia, J. M. Guilarte, and M. S. Plyushchay, Phys. Rev. D **87**, 045009 (2013).

[34] G. Basar, G. V. Dunne, and M. Thies, Phys. Rev. D **79**, 105012 (2009).

[35] J. Q. Liang, H. J. W. Muller-Kirsten, and D. H. Tchrakian, Phys. Lett. B **282**, 105 (1992).

[36] Y. Brihaye, S. Giller, P. Kosinski, and J. Kunz, Phys. Lett. B **293**, 383 (1992).

[37] D. Boyanovsky, H. J. de Vega, R. Holmanm, and J. F. J. Salgado, Phys. Rev. D **54**, 7570 (1996).

[38] P. B. Greene, L. Kofman, A. D. Linde, and A. A. Starobinsky, Phys. Rev. D **56**, 6175 (1997).

[39] G. V. Dunne and K. Rao, J. High Energy Phys. 01 (2000) 019.

[40] F. Finkel, A. Gonzalez-Lopez, A. L. Maroto, and M. A. Rodriguez, Phys. Rev. D **62**, 103515 (2000).

[41] F. Correa, G. V. Dunne, and M. S. Plyushchay, Ann. Phys. (Amsterdam) **324**, 2522 (2009).

[42] F. Correa and V. Jakubsky, Phys. Rev. D **90**, 125003 (2014).

[43] F. Cooper, A. Khare, and U. Sukhatme, Phys. Rep. **251**, 267 (1995).

[44] B. A. Kupershmidt, Phys. Lett. A **102**, 213 (1984).

[45] P. Mathieu, J. Math. Phys. (N.Y.) **29**, 2499 (1988).

[46] M. Chaichian and P. P. Kulish, Phys. Lett. B **183**, 169 (1987).

[47] S. Bellucci, E. Ivanov, and S. Krivonos, J. Math. Phys. (N.Y.) **34**, 3087 (1993).

[48] E. Ivanov, S. Krivonos, and F. Toppan, Phys. Lett. B **405**, 85 (1997); Mod. Phys. Lett. A **14**, 2673 (1999).

[49] F. Toppan, Lect. Notes Phys. **502**, 283 (1998).